

Mathematical modelling of composting processes using finite element method

Pierre Courvoisier

Master student

Department of Bioresource Engineering

McGill University

Montreal, Quebec

2011-02

A thesis submitted to McGill University in partial fulfillment of the requirements of the degree of Msc. of bioresource engineering

©Pierre Courvoisier 2011

ACKNOWLEDGEMENTS

I thank my advisor, Dr.Clark, my labmates, especially Edsel Philip and his answers for my numerous questions, and the friends I had in Montreal. I would like to acknowledge the support of the Natural Sciences and Engineering Research Council of Canada through Discovery Grant number 339814.

ABSTRACT

Composting is one element of waste management. It allows waste to be transformed into a valuable product. The processes involved and the final product, however, may vary in terms of quality, efficiency or security. Models have been established to represent some features of the composting process, but never all of them together. We hypothesized that all the key features from the literature could be gathered in one model. This model should be qualitatively faithful, reliable, and easily adapted to any situation. We used COMSOLTM, software that uses proven algorithms and the finite element method to solve partial differential equations in high spatial resolution in up to three dimensions. The behavior of this model was studied through parameter variations and sensitivity analysis. Patterns in temperature, biomass, substrate, oxygen and water concentration curves were consistent with the typical curves found in literature about composting. Initial water concentration and airflow were found to have an important impact on the composting process, while inlet air temperature did not. The resolution of the mathematical problem in a two-dimensional, longitudinal cross-section of the rectangular vessel allowed the observation of spatial patterns. This model can be used as a basis for further studies as new features are easy to implement. It can likewise be adapted to any apparatus, which makes it useful for comparative analysis. The suggested model, however, has yet to be validated against a physical system and this should be the next step.

ABRÉGÉ

Le compostage est un composant de la gestion des déchets et permet de les transformer en un produit à valeur ajoutée. Les procédés en jeu, ainsi que les produits finis peuvent cependant varier au niveau de la qualité, de l'efficacité, et de la sécurité. Des modèles ont été mis au point pour prendre en compte certaines caractéristiques du compostage, mais jamais de façon exhaustive. Notre hypothèse était que toutes les caractéristiques clés décrites dans la littérature peuvent être réunies en un seul modèle. Ce modèle doit être qualitativement fidèle, fiable, et facilement adaptable à toutes les situations. Nous avons utilisé COMSOLTM, un logiciel qui utilise des algorithmes établis et se base sur la méthode des éléments finis pour résoudre les systèmes d'équations différentielles partielles avec une bonne résolution spatiale en deux ou trois dimensions. La réponse de ce modèle face à des variations paramétriques et à une analyse de sensibilité a été étudiée. Les comportements de la température, de la biomasse, du substrat, de l'oxygène, et de la quantité d'eau ont été cohérents avec ceux trouvés dans la littérature sur le compostage. La concentration initiale en eau, ainsi que l'aération, ont été prouvés avoir un impact important sur le compostage, contrairement à la température de l'air entrant. La résolution du problème mathématique dans une coupe bidimensionnelle longitudinale du container rectangulaire permet l'observation de comportements spatiaux. Ce modèle pourra être utilisé comme un fondement pour de futures études car l'ajout de nouvelles caractéristiques y est aisé. Le modèle peut aussi être facilement adapté à différentes

conditions expérimentales, ce qui en fait un bon outil comparatif. Cependant, le modèle suggéré doit d'abord être validé par des données expérimentales.

TABLE OF CONTENTS

ACKNOWLEDGEMENTS	ii
ABSTRACT	iii
ABRÉGÉ	iv
LIST OF TABLES	x
LIST OF FIGURES	xi
LIST OF VARIABLES	xiv
LIST OF CONSTANTS	xvi
1 Introduction	1
1.1 Waste management	1
1.1.1 A rising realization	1
1.1.2 The production of waste	2
1.1.3 The worth of waste	4
1.1.4 Waste management	5
1.2 Mathematical modelling	8
1.2.1 What is mathematical modelling?	8
1.2.2 Why use mathematical modelling?	10
1.2.3 How to use mathematical modelling?	11
The Blind Men and the Elephant	12
2 Review	16
2.1 Composting	16
2.1.1 Overview	16
2.1.2 Composting phases	16
2.1.3 Heat inactivation	17
2.2 Geometry and experimental apparatus	18

	2.2.1	Geometry	18
	2.2.2	Aeration	19
2.3		Conceptual model	20
	2.3.1	Characterization of the model	20
	2.3.2	A three-phase system	20
	2.3.3	Mathematical conceptualization	21
	2.3.4	Apparatus	22
	2.3.5	Spatial dependency	22
	2.3.6	Finite Element Method	23
2.4		Compost	23
	2.4.1	Moisture content	23
	2.4.2	Residual water content	25
	2.4.3	Bulk density	25
	2.4.4	Porosity	26
	2.4.5	Interactions	26
2.5		Biomass processes	26
	2.5.1	Biomass population	26
	2.5.2	Main equation	28
	2.5.3	Impact functions	28
	2.5.4	The impact of biomass on other variables	32
2.6		The substrate	32
	2.6.1	Main equation	33
	2.6.2	Different types of substrate	33
2.7		Physical processes	34
	2.7.1	Porous media	34
	2.7.2	Fluid dynamics	34
	2.7.3	Heat transfer equations	36
	2.7.4	Diffusion	37
	2.7.5	Mass transfer across interfaces	38
	2.7.6	Water equations	39
	2.7.7	Oxygen equations	40
2.8		Other processes	40
2.9		Sensitivity	41
	2.9.1	Stochastic methods	41
	2.9.2	Deterministic methods	42
	2.9.3	Sensitivity of compost models	42

3	Methodology	44
3.1	Description of mathematical modelling	44
3.2	Geometry	45
3.3	The solver	47
3.4	The compost	47
	3.4.1 Overview	47
	3.4.2 A three-phase system	48
	3.4.3 A porous medium	48
3.5	The biomass	49
	3.5.1 Main equation	49
	3.5.2 Impact functions	50
3.6	The substrate	55
	3.6.1 Main equation	55
	3.6.2 Initial conditions	56
	3.6.3 Boundary conditions	56
3.7	Physical processes	56
	3.7.1 Main equation	56
	3.7.2 Diffusion in porous media	57
	3.7.3 Fluid dynamic equations for the gas phase	58
	3.7.4 Enthalpy of air	61
	3.7.5 Heat equations in the liquid phase	63
	3.7.6 Water equations for gas and liquid phases	66
	3.7.7 Oxygen equations for liquid and gas phases	71
3.8	Other processes	76
3.9	Sensitivity analysis	76
	3.9.1 Definition and goals	76
	3.9.2 Method	77
3.10	Assumptions	80
4	Results	82
4.1	General behavior	82
	4.1.1 Temperature	82
	4.1.2 Biomass	86
	4.1.3 Substrate	89
	4.1.4 Oxygen	91
	4.1.5 Water	93
4.2	Impact of initial concentration of water	96

4.2.1	Experimental procedure	96
4.2.2	Higher initial concentration	96
4.2.3	Low initial moisture content	97
4.2.4	Effect of initial moisture content on final substrate density	98
4.3	Impact of airflow	99
4.3.1	Experimental procedure	99
4.3.2	Higher airflow	99
4.3.3	Lower airflow	100
4.3.4	Effect on the bulk temperature	103
4.4	Sensitivity analysis	103
4.4.1	Consumption of substrate	103
5	Discussion	107
5.1	Multiphysics	107
5.2	A configurable model	107
5.3	Spatial dependency	109
5.4	Further improvements	110
5.5	Sensitivity analysis	111
	BIBLIOGRAPHY	112

LIST OF TABLES

<u>Table</u>		<u>page</u>
1	Variable names	xiv
2	Constant names	xvi
2-1	Impact functions	29
4-1	Sensitivity analysis results	105

LIST OF FIGURES

<u>Figure</u>	<u>page</u>
1-1 Total municipal waste production by households, institutions and business, except for industry and agriculture, in the US from 1960 to 2000. Picture adapted from Katz (2002)	3
1-2 Waste generation from different sources in Canada (in kilotonnes), 2002 according to Anonymous (2004)	4
1-3 Changes in methods of municipal waste management in the US from 1960 to 2000. Adapted from Katz (2002).	7
1-4 Waste disposal and diversion of non-hazardous waste in Canada in 2002 and 2004 (Anonymous, 2004).	8
2-1 Impact functions of temperature used by Nielsen and Berthelsen (2002) (a), Stombaugh and Nokes (1996) (c), and Rosso et al. (1993) (b and d for different ranges of temperature).	30
3-1 Schematic of a closed composting vessel. The compost is represented by the shaded area. It is supported by a mesh that is fine enough to prevent the compost from falling, yet coarse enough to let the air pass through. Fresh air is supplied through the inlet duct vent and exhausted through the lid.	46
3-2 Schematic of a porous medium. The solid particles are covered by a water film. Depending on the moisture content, some empty pore space will be left for the air to circulate.	49
3-3 Impact of the amount of water on the water exchange between the gas and liquid phase. For this study, the residual water content considered was 400 mol m^{-3} . For low water concentration, surface tension reduces the amount of water exchanged.	70

3-4	Schematic illustrating the two-film theory. The curves are the plots of the partial distributions of partial pressure and concentration of a species in the different phases at the interface. The mass flux is as indicated. Adapted from Cussler (1997)	73
4-1	Pattern of variation of bulk temperature with time at several heights in the center of the rectangle representing the composting bed.	83
4-2	Pattern of variation of gas temperature with time at several heights in the center of the composting bed.	84
4-3	Pattern of variation of bulk temperature in a vertical slice of the compost bed.	85
4-4	Pattern of variation of biomass concentration with time at several heights in the center of the composting bed.	87
4-5	Pattern of variation of biomass concentration with respect to height, in a vertical slice of the compost bed. Day 6 is not shown because the biomass concentration on day 6 was very small in comparison to days 10, 13 and 17.	88
4-6	Pattern of variation of substrate density with time at several heights in the center of the compost bed.	89
4-7	Pattern of variation of substrate density in a vertical slice of the composting bed. The gradient in the substrate density was extremely large, ranging from 200 kg m^{-3} to zero in few centimeters, so the mesh size of the finite element mode was not small enough to smoothly capture the variation of the substrate. Hence, the small white band represents mesh elements where the gradient was so strong that the solver gave a negative solution. A smaller mesh size would have solved this problem, but such a change would also have greatly increased the time required for the simulations.	90
4-8	Pattern of variation of dissolved oxygen in water with respect to time at several depths in the center of the compost bed.	91
4-9	Pattern of variation of oxygen in the gas phase with respect to time at several depths in the center of the compost bed.	92

4-10	Pattern of variation of dissolved oxygen in water with respect to height in a vertical slice of the compost bed.	93
4-11	Pattern of variation of water vapor with respect to time at several depths in the center of the compost bed.	94
4-12	Pattern of variation of liquid water with time at several heights in the center of the composting bed.	95
4-13	Final spatial distribution of bioavailable substrate concentration with regards to different initial concentration of water. The initial concentrations of water are indicated in proportion of the value from Table 2. The concentration of substrate is sometimes negative close to the highest gradient of water concentration. This phenomenon is due to the fact that the mesh size was too great to smoothly capture the variation of the substrate. Reducing the mesh size would solve the problem but increase the simulation time.	98
4-14	Biomass concentration resulting from a low differential pressure at the inlet ($10 Pa$) after 60 days. The pattern of concentrated biomass is shaped like a U.	102
4-15	Bulk temperature in the compost for various differential pressures at the inlet.	103

Table 1: LIST OF VARIABLES

Symbol-unit	Name
$C_{compost} (J kg^{-1} K^{-1})$	Heat capacity of compost
$\vec{F} (kg m^{-2} s^{-2})$	Gravitational force per unit of volume
$f_{O_2dis} (unitless)$	Impact function of the oxygen availability on growth rate
$f_T (unitless)$	Impact function of the temperature on growth rate
$f_{H_2Oliq} (unitless)$	Impact function of the water availability on growth rate
$H_2O_{gas} (mol m^{-3})$	Concentration of water vapor in the gas phase
$H_2O_{liq} (mol m^{-3})$	Concentration of liquid water in the liquid phase
$J_w (m s^{-1})$	Flux of water in the porous medium
$MC_{d.b.} (unitless)$	Moisture content (dry basis)
$MC_{vol} (unitless)$	Volumetric moisture content
$MC_{w.b.} (unitless)$	Moisture content (wet basis)
$O_{2consumption} (mol m^{-3} s^{-1})$	Oxygen consumption term by the biomass
$O_{2ex} (mol m^{-3} s^{-1})$	Oxygen exchange term between the two phases
$O_{2gas} (mol m^{-3})$	Concentration of oxygen in the gas phase
$O_{2dis} (mol m^{-3})$	Concentration of dissolved oxygen in the liquid phase
$p (Pa)$	Air pressure
$psat (Pa)$	Saturated vapor pressure of water in the gas phase
$Q_{bio} (W m^{-3})$	Heat released by the biomass
$Q_{ex} (W m^{-3})$	Heat exchange between gas and liquid phase

Continued on next page

Table 1 – continued from previous page

Symbol-unit	Name
$S (kg m^{-3})$	Substrate concentration
$T (K)$	Air temperature
$\vec{u} (m s^{-1})$	Velocity vector of the gas phase
$W_{ex} (mol m^{-3})$	Water exchange term between the two phases
$X (kg m^{-3})$	Biomass concentration
$X_{O_2liq} (unitless)$	Molar fraction of the oxygen in the liquid phase
$\mu (s^{-1})$	Growth factor of the biomass
$\rho (kg m^{-3})$	Air density
$\rho_{liq} (kg m^{-3})$	Bulk density density
$\theta (K)$	Bulk temperature

Table 2: LIST OF CONSTANTS

Symbol	Value	Definition	Reference
A	4.6507	unitless	
a	$0.065 K^{-1}$	Scaling coefficient of temperature function	Nielsen and Berthelsen (2002)
b	$0.45 K^{-1}$	First parameter of temperature function	Nielsen and Berthelsen (2002)
c_{H_2O}	$32.13 J mol^{-1} K^{-1}$	Second parameter of temperature function	Perry and Green (2007)
C_{NVS}	$25.18 kg m^{-3}$	Specific heat capacity of water vapor	Stombaugh and Nokes (1996)
$D_{H_2O_{gas}}$	$2.55 \times 10^{-5} m^2 s^{-1}$	Non volatile solids concentration	ASHRAE (2009)
$D_{O_2_{gas}}$	$2.06 \times 10^{-5} m^2 s^{-1}$	Diffusion coefficient of water (gas)	ASHRAE (2009)
$D_{O_2_{dis}}$	$2.10 \times 10^{-9} m^2 s^{-1}$	Diffusion coefficient of oxygen (gas)	Cussler (1997)
g	$9.81 m s^{-2}$	Diffusion coefficient of oxygen (liq) at 25°C	
$[H_2O]$	$55.56 mol L^{-1}$	Acceleration due to gravity	
$H_2O_{liq_{ini}}$	$20055 mol m^{-3}$	Concentration of pure water	
h_{trans}	$868 W m^{-3} K^{-1}$	Initial amount of water	Stombaugh and Nokes (1996)
k_d	$0.025 h^{-1}$	Convective heat transfer coefficient	Petric and Selimbasic (2008)
k_{LaO_2}	$2.71 \times 10^{-5} mol s^{-1} Pa^{-1} m^{-3}$	Death rate of microorganisms	Stombaugh and Nokes (1996)
		Mass transfer coefficient of oxygen	Petric and Selimbasic (2008)

Continued on next page

Table 2 – continued from previous page

Symbol	Value	Definition	Reference
k_{Law}	$4.82 \times 10^{-5} \text{ mol s}^{-1} \text{ Pa}^{-1} \text{ m}^{-3}$	Mass transfer coefficient of water	Petric and Selimbasic (2008)
k_{liq}	$0.2 \text{ W m}^{-1} \text{ K}^{-1}$	Thermal conductivity of compost	Ahn et al. (2009); Chandrakanthi et al. (2005)
K_{O_2}	$0.07124 \text{ mol m}^{-3}$	Oxygen saturation constant	adapted from Stombaugh and Nokes (1996)
K_s	62 kg m^{-3}	Substrate saturation constant	Stombaugh and Nokes (1996)
L_{vap}	40660 J mol^{-1}	Latent heat of evaporation of water	Bitton (1998)
M_{air}	29 g mol^{-1}	Molar mass of air	
M_{H_2O}	18 g mol^{-1}	Molar mass of water	
p_0	$101,325 \text{ Pa}$	Initial pressure	
R	$8.314 \text{ J K}^{-1} \text{ mol}^{-1}$	Perfect gas constant	Bitton (1998)
S_0	215.7 kg m^{-3}	Initial substrate density	Stombaugh and Nokes (1996)
T_0	313 K	First temperature constant	Nielsen and Berthelsen (2002)
T_1	343 K	Inflection point temperature	Nielsen and Berthelsen (2002)
T_{ini}	21°C	Initial temperature	

Continued on next page

Table 2 – continued from previous page

Symbol	Value	Definition	Reference
U	$0.278 \text{ J K}^{-1} \text{ s}^{-1} \text{ m}^{-2}$	Overall heat transfer coefficient of walls	Liang et al. (2004)
X_0	0.008 kg m^{-3}	Initial microorganism cell mass concentration	Stombaugh and Nokes (1996)
$Y_{O_2 \rightarrow S}$	$42.81 \text{ mol kg}^{-1}$	Yield coefficient of consumption of oxygen by the biomass	Stombaugh and Nokes (1996)
$Y_{S \rightarrow w}$	$35.05 \text{ mol kg}^{-1}$	Yield coefficient of creation of water by the biomass	Stombaugh and Nokes (1996)
$Y_{X \rightarrow S}$	$-0.35 \text{ kg X kg S}^{-1}$	Yield coefficient of biomass growth	Stombaugh and Nokes (1996)
ΔH	$1.54 \times 10^7 \text{ J kg}^{-1}$	Reaction enthalpy of substrate combustion	Van Ginkel (1996)
Δp	300 Pa	Inlet difference in pressure	Stombaugh and Nokes (1996)
ϵ_t	0.8 unitless	Porosity of compost	Agnew and Leonard (2003)
κ	10^{-10} m^2	Permeability of compost	Poulsen and Moldrup (2007)
μ	0.2 h^{-1}	Maximum specific growth rate of microorganisms	Stombaugh and Nokes (1996)
ν_{max}	$0.48 \text{ kg}_{substrate} \text{ kg}_{biomass}^{-1}$	Maximum microbial maintenance coefficient	Stombaugh and Nokes (1996)

Continued on next page

Table 2 – continued from previous page

Symbol	Value	Definition	Reference
ρ_0	1.29 kg m^{-3}	Density of air at standard condition	Cutnell and Johnson (2005)
ρ_w	1000 kg m^{-3}	Density of water	ASHRAE (2009)

CHAPTER 1 Introduction

1.1 Waste management

1.1.1 A rising realization

Waste management has been an issue of increasing importance over the years since first regulations appeared. About 30 years ago, in the United States, the responsibility for waste disposal switched from the local level to the state and national levels, thus causing regulation issues (Benjamin, 2010). One of the most famous stories of waste disposal is the journey of the *Mobro*.

The *Mobro* was a barge filled with 3,200 t¹ of New York trash, which embarked in March, 1987. The waste was at first intended to go to a landfill in Louisiana. In order to save some money, however the owner of the barge tried to unload its waste in North Carolina. He tried to hurry the process, and a local official feared that this rush was due to the presence of hazardous waste in the cargo. This rumor spread quickly and the barge was rejected by six states and three countries in an odyssey that lasted 162 days and over 6,000 miles (Gutis, 1987). The cost of this mess was about 1 million dollars for the operator of the boat (Gutis, 1987).

¹ Throughout the document, t will refer to a tonne: 1,000 kg.

Public awareness in the United States was increased due to this crisis. It became recognized that poor waste management can cause two phenomena (Rogaume, 2006):

- Waste can be publicly perceived as a source of aesthetic, olfactory, and noise pollution;
- Waste can engender environmental impacts that must be dealt with, such as the impairment of soil and air quality, or the proliferation of pests.

1.1.2 The production of waste

It is commonly stated that the world production of waste per capita has constantly increased over the last century. Katz (2002) mentions, however, that modern household production of waste per person has not risen a lot since early 20th century, when coal ash and horse manure were a significant part of waste production. Other sources of waste, like industry or institutions, however, did increase, as shown in Fig. 1–1. Municipal waste production more than doubled during this period. Domestic waste production per capita increased less rapidly over the same interval (Katz, 2002).

At the global scale, the United Nations (Anonymous, 2009) provides data on municipal waste collected according to national surveys up to 2009. This source estimates that 916 million t of waste were collected in the world in 2009. It also lists the amount of waste that was landfilled, incinerated, recycled or composted.

The total production of all kinds of waste in Canada rose from 29.3 million t in 2000 to 30.45 million t in 2002 (Anonymous, 2005). This figure, when normalized according to the population of Canada, gives a yearly production of waste of 971 kg

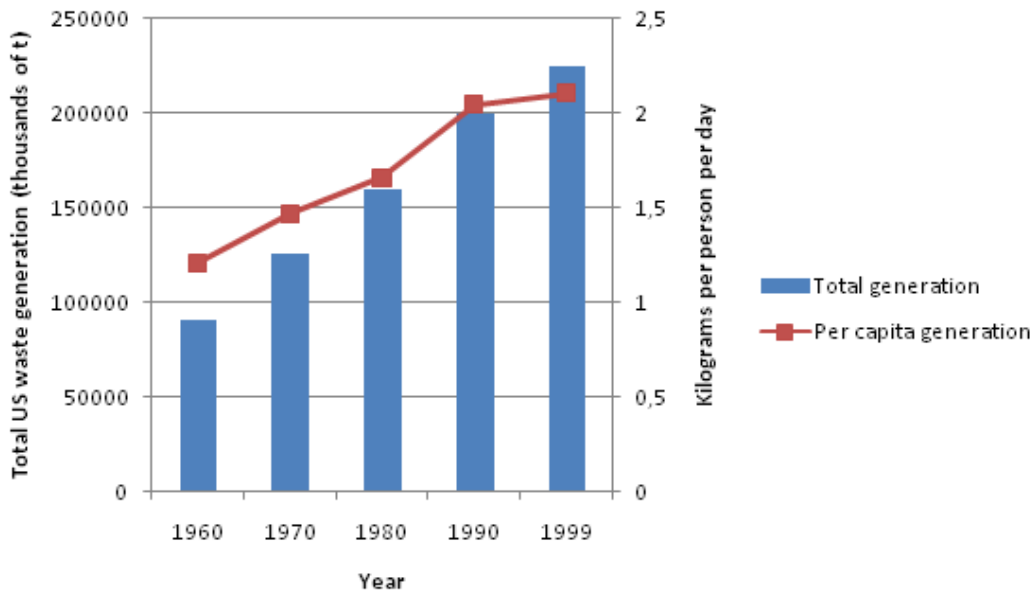


Figure 1–1: Total municipal waste production by households, institutions and business, except for industry and agriculture, in the US from 1960 to 2000. Picture adapted from Katz (2002)

per person in 2002. The total increase in waste generation over the two years was almost 2% per year.

The division of this waste according to residential, industrial and construction sources is shown in Fig. 1–2. Almost half of the waste generated in Canada comes from industrial, commercial and institutional sources, whereas the contribution of construction, renovation and demolition is relatively small. The majority of waste generated by households was organic material (40% of total generated waste) and paper (26% of total generated waste).

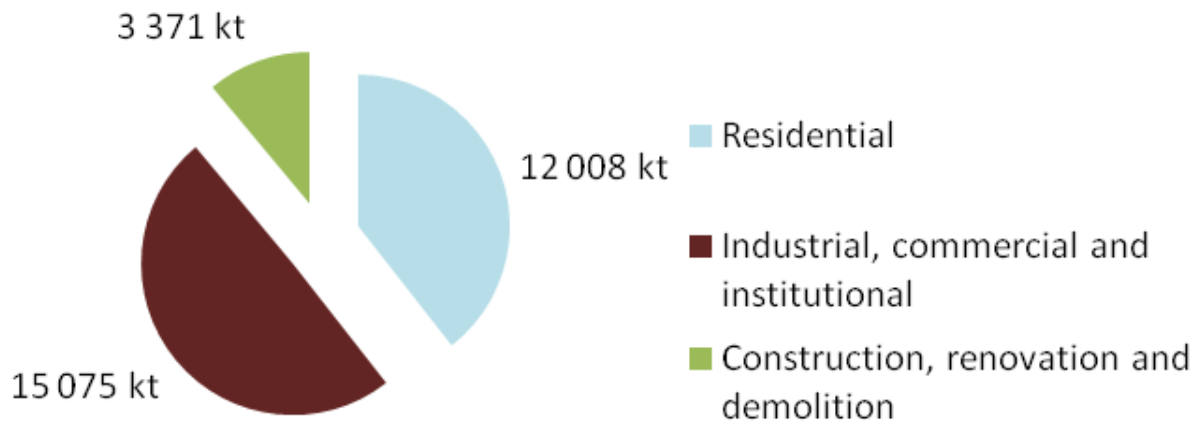


Figure 1–2: Waste generation from different sources in Canada (in kilotonnes), 2002 according to Anonymous (2004)

1.1.3 The worth of waste

According to the proverb, “One man’s garbage is another man’s treasure”. Waste is indeed a considerable source of raw material and energy. Indeed, all the expensive materials used in the fabrication of products could theoretically be extracted from those products once they reach their end-of-life. The difficulty of extracting those materials or energy, however, necessitates complex and expensive techniques that are not competitive yet compared to the use of new raw materials. Yet, according to Johnson et al. (2006), 2.6 million tons of chromium were discharged by industry in 2006, while 2.95 million t were produced from mining activities. As for copper, in 1994, 1.8 million t of copper was discarded in landfills in products at their end-of-life (Lifset et al., 2002) while global production was 10 million t according

to Dzioubinski and Chipamn (1999). Similar figures could be obtained for other metals, but these show that the amount of raw materials in waste is not trivial, and that recycling could be improved by a tremendous margin.

The reuse of raw materials in end-of-life products is not the only way to valorize waste. Waste often has high energy content that may be recoverable through combustion (Rogaume, 2006). This is subject to the condition that the techniques used to control pollution from the combustion not be too expensive.

Organic waste can also be considered as feedstock for composting. Composting generates a humus-like product, which can be a beneficial soil ammendment and nutrient source.

1.1.4 Waste management

Waste management takes care of wastes from the time they are generated to their end-of-life. The easiest way to manage waste is to accumulate it in landfills and wait for microorganisms and time to process it. There is no control in this option, however, and it generates pollution and takes a relatively long time: the current rate of waste generation exceeds the rate of total degradation in landfills.

Burning waste is a rapid and convenient process. Nevertheless, the environmental toll is often unacceptable and unjustified by the net recovery of energy. Even though landfills and incinerators have long been the most common way to take care of waste, their finite capacities and pollution risks encourage the use of recycling.

Recycling is the process whereby a material (e.g., glass, metal, plastic, paper) is diverted from the waste stream and remanufactured into a new product, or is used as a raw material substitute (Anonymous, 2004). It should be mentioned that

sometimes the recycling methods for specific wastes are so expensive or so environmentally unfriendly, through the use of chemical processes, for instance, that they are not commonly used.

Composting is the equivalent of recycling for organic waste. Biological degradation of organic waste is a part of the “circle of life”, and thus has existed for as long as organic matter. As early as the Neolithic Period, waste pits were used to process organics for eventual application on agricultural fields (Martin and Gershuny, 1992). Later on, early civilizations in South America, India, China and Japan were known to use animal and human residue as fertilizers (Howard, 1945). Those residues were left to rot in pits for long periods before being used. Industrial composting, however, was developed recently. One of the first scientific analyses of large-scale composting operations took place in India in 1933 (Howard, 1936). Since then, composting has been improved and recognized as a reliable way to divert organic wastes from conventional disposal and to valorize them.

In the United States, the use of recycling and composting has gradually increased over the last century. This trend can be seen in Fig. 1–3, which shows that the use of recycling and composting in place of landfilling and combustion has been increasing since 1990.

In many countries, the disposal of waste in any form, e.g. landfilling, recycling, is taken care of by both public and private facilities. In Canada in 2000, disposal among these two categories was about equal, with 12.9 million t and 10.2 million t of waste disposed of by public and private plants, respectively (Anonymous, 2005).

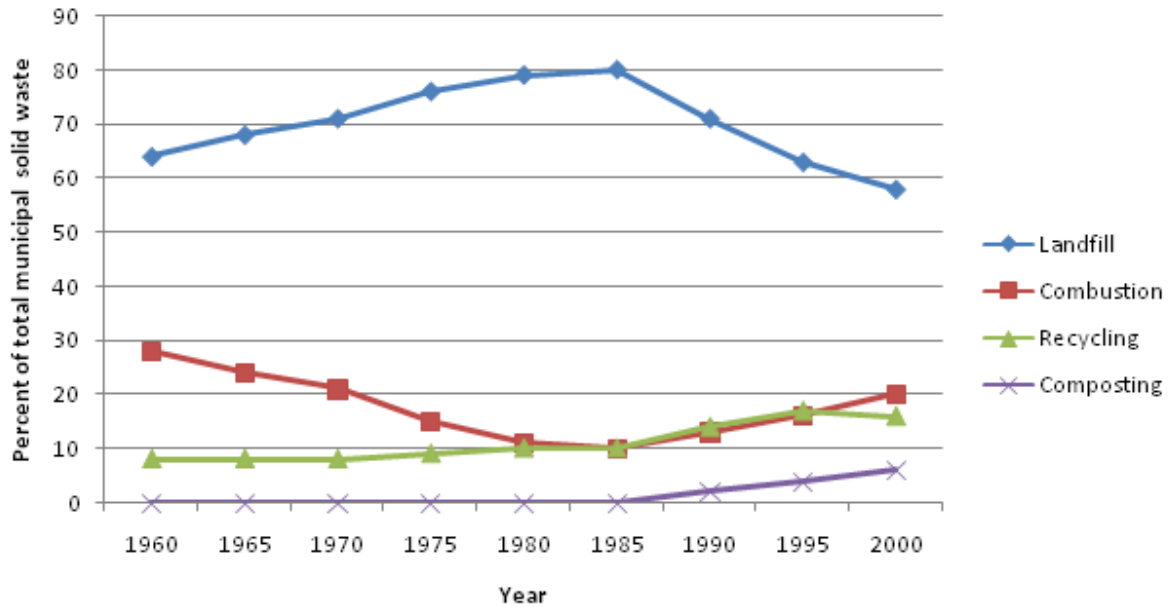


Figure 1-3: Changes in methods of municipal waste management in the US from 1960 to 2000. Adapted from Katz (2002).

Diverted waste is the material that is redirected from disposal facilities and represents the sum of all materials processed for recycling or reuse at an off-site recycling or composting facility. The proportion of diverted waste in Canada in 2002 and 2004 can be seen in Fig. 1-4. The amount of disposed and diverted waste between 2002 and 2004 seems to be the same in relative terms, but the proportional increase over the two years was, respectively, 2.8% and 18.8%.

The waste management business employed about 24,000 people in Canada in 2004 for a total expenditure of \$1.544 billion (Anonymous, 2004).

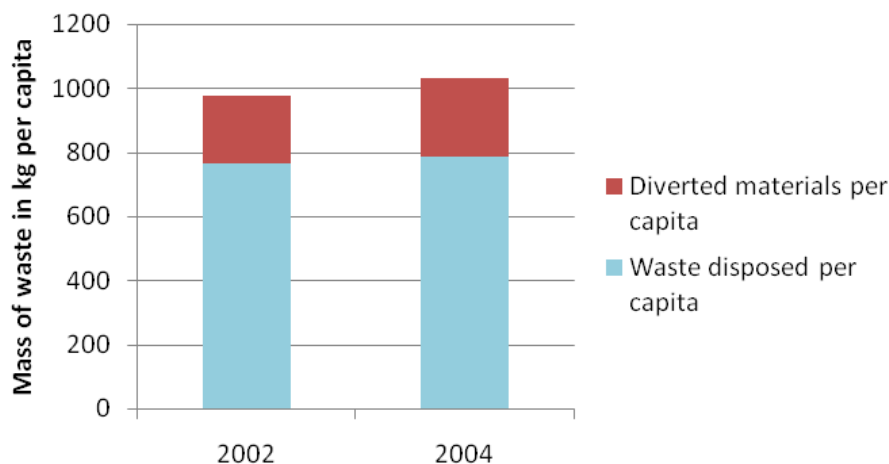


Figure 1–4: Waste disposal and diversion of non-hazardous waste in Canada in 2002 and 2004 (Anonymous, 2004).

1.2 Mathematical modelling

1.2.1 What is mathematical modelling?

The specific meaning of *model* may vary with circumstances, but a common definition is something that mimics relevant features of the situation being studied (Bender, 1978). Mathematics are formal and concise means of describing patterns, and so are used to model processes in every field of science, and in many other areas of application. For instance, mathematics are applied in economics, biology, linguistics, transport, industry, business, and government (Berry and Houston, 1995).

Physics and mathematics strongly interact, as recent physical theories employ the most recent mathematical theories (Bochner, 1966). This phenomenon can also be seen in other sciences, such as biology and social sciences: the recent mathematical needs from these sciences have pressed mathematicians to develop new theories.

Working with mathematical models does not just require mathematical skills. One must be able to adapt to the field of application, because information about the system to be modelled is often in a non-mathematical form, and the interpretations of models must also be communicated in a non-mathematical form. Mathematical modelling lies, therefore, between the reception of the information and the delivery of the results (Berry and Houston, 1995).

Bender (1978) states that “*a mathematical model is an abstract, simplified, mathematical construct related to a part of reality and created for a particular purpose*”. In the context of a mathematical model, phenomena can be divided into three classes (Bender, 1978):

- The things with negligible impact on the system of interest, for instance the gravitational attraction of the moon on a skier.
- The inputs to the model: things that do have an effect on the model but that are considered as external to the model. An example might be the gravitational attraction of the earth on a skier or the friction coefficient of the ski on the snow.
- The outputs of the model: the things the model was designed to study. For example, the position of a skier on a snow slope.

The classification of all the things in the universe into those three categories is a fundamental element of a model because it helps to define the question that the model will answer: *What are the effects of those – and only those – things on these – and only these – things?* Formally a mathematical model should be structured to answer

a single specific question. In order to solve a real-life problem using mathematical modelling, the mathematical terms of the question must be chosen carefully: what to neglect, and why to neglect them. Sometimes, because of complexity, modelers will neglect a factor that is actually quite important to the understanding of their real-life problem. The result of the mathematics will then unrealistic. When the result is not what common sense predicted, however, it could be that the effects taken into account generate a response pattern that no one has been able to foresee, which is a good discovery. Such a result, however, is more commonly due to a poor conceptualization of the actual problem in mathematical terms.

One should be careful when interpreting the results of a mathematical model. The application of mathematical theory only provides a mathematical system or construct which, if correct, is internally consistent with the axioms and theorems that have been used in its formulation. In order for such a mathematical system to be applied as a model, however, there must be some interpretation of the construct with respect to the degree that it shares some interesting features with the physical system that it is presumed to describe. Such an interpretation, though necessary, is prone to subjectivity: e.g., the imposition of personal bias or unfounded conjecture or extrapolation on the part of the people who are making the interpretation.

1.2.2 Why use mathematical modelling?

We can start by wondering what makes mathematical models useful in the first place. Bender (1978) states that the mathematical syntax gives access to many simplifications:

- The mathematical formulation is precise and leaves no room for implicit assumptions to go unnoticed.
- The conciseness of mathematical language enhances the manipulation of concepts.
- The mathematics toolbox contains a huge number of theorems that can be of great help, if used in the right situation.
- Mathematics is well suited to computer simulations and allows high speed calculations in order to solve problems in their mathematical form.

The third and fourth items however do not work in the same direction: Theorems are useful to find general conclusions with simple models while computers generate specific answers for complicated models. This is because theorems deal with abstract logic while computational models handle numerical calculations.

One utility of mathematical modelling is that it enables the modeler to make predictions about a topic without any physical test, which can be useful, for instance, when modelling nuclear explosions or if the duration of an experiment is too long (or unethical, expensive, etc...) to be able to reproduce it as required.

1.2.3 How to use mathematical modelling?

Mathematical modelling proceeds in three main steps (Berry and Houston, 1995).

- The real world problem is cast in a mathematical form. This process, along with the definition of assumptions, characterizes the mathematical model.

- The mathematical model is solved, by the use of theorems or numerical computations.
- The solution of the mathematical model is translated back into the original context. The results obtained can then be interpreted in order to solve the real problem.

The formulation of the model depends on the modeler, as he is the one who will decide which features to take into consideration and which not to. In order to have a good model, a good modeler is needed. The qualities of such an individual are open-mindedness, creativity, a holistic perspective, and the ability to communicate clearly, especially with the people familiar with the field of the problem (Bender, 1978). The poem from John Godfrey Saxe (1816-1887) illustrates this line of thought by counter-example:

The Blind Men and the Elephant

It was six men of Indostan
 To learning much inclined,
Who went to see the Elephant
 (Though all of them were blind),
That each by observation
 Might satisfy his mind.

The First approached the Elephant,

And happening to fall
Against his broad and sturdy side,
At once began to bawl:
“God bless! but the Elephant
Is very like a wall!”

The Second, feeling of the tusk,
Cried, “Ho! what have we here
So very round and smooth and sharp?
To me 'tis mighty clear
This wonder of an Elephant
Is very like a spear!”

The Third approached the animal,
And happening to take
The squirming trunk within his hands,
Thus boldly up and spake:
“I see,” quoth he, “The Elephant
Is very like a Snake!”

The Fourth reached out an eager hand,
And felt about the knee.
“What most this wondrous beast is like
Is mighty plain,” quoth he;
“'Tis clear enough the Elephant

Is very like a tree!”

The Fifth who chanced to touch the ear,

Said: “E’en the blindest man

Can tell what this resembles most;

Deny the fact who can,

This marvel of an Elephant

Is very like a fan!”

The Sixth no sooner had begun

About the beast to grope,

Than, seizing on the swinging tail

That fell within his scope,

“I see,” quoth he, “the Elephant

Is very like a rope!”

And so these men of Indostan

Disputed loud and long,

Each in his own opinion

Exceeding stiff and strong.

Though each was partly in the right

And all were in the wrong!

John Godfrey Saxe (1816-1887)

The creation of the model is often not an easy task. The first step is to formulate the problem. The formulation will depend on the answer of the modeler to: “what do I

want the model to do?”. This is a complex task for, as Poul Anderson, an American science fiction writer, is widely quoted as having said “*I have yet to see any problem, however complicated, which, when looked at in the right way, did not become still more complicated*”. This sentiment applies well to the world of mathematic modelling, especially when the modeler is unsure of the process underlying the system that he is trying to model.

The variables chosen by the modeler are categorized as mentioned earlier – neglected, inputs, outputs – and their relations are defined.

Once the model is defined, the verification begins, where the modeler checks all the parts of the model in order to discover possible mistakes. Finally, the model needs to be validated. The validation ensures that the model behaves as planned, usually by testing the model against simple case scenarios where the modeler knows what to expect. Afterwards, the model is ready to use in simulations.

It is to be noted that “*it is not possible to maximize simultaneously generality, realism, and precision*” (Levins, 1968). The generality is the possibility of applying the results to other problems, the realism stands for the meaning of the mathematical answer as it relates to the real-life problem, and the precision is that of the mathematical answer. The modeler should understand which of these three aspects are required in order to yield the most appropriate answer.

CHAPTER 2

Review

2.1 Composting

2.1.1 Overview

Composting is the activity of gathering organic waste in one same place, in a pile, for instance, to let the biomass within it degrade over time. It takes between weeks and months for the full process to be completed. The compost process in a factory is purposefully aerobic, for it is faster, cleaner, prevents the emission of noxious gases, and provides a humus of better nutritive quality as compared to anaerobic processes.

2.1.2 Composting phases

At the beginning of the composting process the temperature will quickly rise from ambient as high energy, easily degradable compounds like sugar or protein are metabolized (Diaz, 2007). While the compost is still below 40°C it is said to be in the mesophilic phase.

The microorganisms that raise the temperature from ambient have difficulty adapting to temperatures greater than 40°C. Other organisms will dominate during the higher temperatures up to 60-70°C. This high temperature phase is called the thermophilic phase. The remaining easily-degradable compounds will be consumed during this phase. This phase is important because the high temperatures inactivate pathogens and kill most of weed seeds and insect larvae (Diaz, 2007).

The thermophilic phase is followed by a second mesophilic phase (Diaz, 2007). This third phase sees the beginning of the degradation of the most resistant organics (Haug, 1993). As all the high energy substrates have already been consumed, the temperature decreases, and the compost enters the curing phase (Diaz, 2007).

The compost is stabilized during the maturation phase, which includes the mineralization of slowly degradable molecules and the humification of ligno-cellulosic compounds (Diaz, 2007). The composting process is often stopped during curing, however; otherwise, all of the organic matter would be mineralized and the resulting material would be less useful.

The quality of the resulting compost may be assessed according to several features such as particle size distribution, moisture content, texture, odor, and general appearance (Haug, 1993). The stability or maturity of compost can be evaluated by the oxygen consumption rate, the absence of phytotoxic compounds, or the reduction of the biodegradable solids.

2.1.3 Heat inactivation

Compost feedstock may potentially carry human, animal or plant pathogens as well as unwanted biological agents like weed seeds and insect eggs (Haug, 1993). Compost cannot be used to fertilize soil before these elements are inactivated. Fortunately, these biological agents are naturally destroyed or deactivated through thermophilic composting due to the denaturation of proteins by heat (Haug, 1993). The length of exposure to elevated temperature is important to ensure that all or most of the pathogens are inactivated.

2.2 Geometry and experimental apparatus

Many composting systems of the following types are described in detail in Haug (1993), along with an historical review.

2.2.1 Geometry

The geometry of a compost bed is usually a pile, windrow or contained in a vessel. Most of the studies about compost used vessels or windrows since the latter are more commonly used at industrial scales.

Windrow. Windrows are the more common configuration for non-reactor systems (Haug, 1993), whereby waste is formed into a row and turned periodically. Aeration can be natural, through buoyancy forces, or forced, by blowers. The only mixing occurs along the height and width. Some mathematical models of windrows have been developed (Bongochgetsakul and Ishida, 2008).

Pile. Static piles of compost are turned infrequently or not at all. They are more often aerated than are windrows. Glancey and Hoffman (1994) list physical properties of static compost piles for different types of feedstock (e.g. coefficient of friction, angle of repose, etc). Few models have been developed because of the challenges posed by irregular shape.

Vessel. Reactors are often aerated, either by vertical or horizontal aeration (Haug, 1993). Reactors can be easily adapted to a laboratory scale and also easily instrumented with sensors, and thus are often the subjects of experiments and mathematical modelling (Chandrakanthi et al., 2005; Ekinici, 2004; Liang et al., 2004; Lin et al., 2007; Mayo, 1997; Miller, 1989; Petric and Selimbasic, 2008; Sole-Mauri et al., 2007; Stombaugh and Nokes, 1996).

2.2.2 Aeration

The supply of oxygen is critical in composting and there are several ways to regulate it.

Turning. Turning as an aeration method has not often been modelled as it involves a discontinuity over time, which is always complicated to handle mathematically. The approach, therefore, is often to solve separately between two turning events and to use rules to estimate changes in the properties of the compost in order to model the turning process (Bongochgetsakul and Ishida, 2008).

Passive aeration. To be efficient, compost needs a supply of oxygen to ensure aerobic conditions. Turning and forced aeration can be used. Natural conditions, however, may be used too, as buoyancy forces will move the air as the biomass heats up. Yu et al. (2005) reported that passive aeration can generate airflow from 0.007 to 0.07 ($m\ min^{-1}$).

Forced aeration. Mechanical aeration is the most common way to supply oxygen to the biomass, as it is constant and reliable. Aeration may be described in terms of airflow rate (Stombaugh and Nokes, 1996) or pressure difference (Miller, 1989). The inlet air flow rate is often used to control the characteristics of the air entering the compost, such as temperature or humidity ratio, and sampling is generally done at the exhaust. Closed-loop reactors have also been built, wherein the exhaust pipe is connected to the inlet through a duct (Sole-Mauri et al., 2007).

2.3 Conceptual model

2.3.1 Characterization of the model

Compost models are complex because they include equations and constants from different fields of science: e.g. physics, chemistry, and biology. Parameters belong to three main categories (Mason, 2006):

- Those describing fundamental properties of air, water and insulating materials;
- Those describing the raw composting material characteristics;
- Those relating to substrate degradation rates and microbial growth.

The number of parameters varies largely from one model to another. The simplest ones use only about 6 parameters, while the most complex can employ up to 30.

The main state variables are temperature, moisture content, oxygen, and biomass. Many other variables can be implemented, however, like airflow, carbon-to-nitrogen ratio, or carbon dioxide emission rate (Mason, 2006). Some aspects of a system complex to be described analytically. For instance, the geometry of every pore of the compost bed cannot be taken into account, for such a description would overwhelm the available computational capacity. A description of average, or bulk properties is then used, and parameters such as porosity are defined to characterize it. Chemical and biological processes are similarly averaged. Hence, the equations used in compost models are often empirical, or are simple functions, like Monod or first-order equations.

2.3.2 A three-phase system

Compost is a three-phase system: solid (feedstock), liquid (water film) and gas (air). Not all of these phases, however, are necessarily represented in a model. Some

studies (Stombaugh and Nokes, 1996) have modelled only the gas phase, which is responsible for all the mass exchange with the exterior.

More complex models have represented two phases – liquid and gas – in order to model the mass exchange between them (Petric and Selimbasic, 2008).

The most elaborate models implement the solid phase and its solubilization into the water film surrounding the particles (Sole-Mauri et al., 2007). According to Haug (1993), the process of solubilization is a significant rate-controlling mechanism.

2.3.3 Mathematical conceptualization

As mentioned, it is important to explicitly state one’s modelling objectives, and to refer back to them once the resulting model is built (Hamelers, 2004).

The values of most composting parameters are not well known and it is the role of the modeller to choose those which will fit the best the model.

Most of the current models are inductive: they directly relate inputs such as temperature to outputs such as growth rate in a specific scenario. Such an empirical approach is useful when the underlying mechanisms are not perfectly known. A problem with such an approach is that it does not apply well to other scenarios. Thus, to be accurate, those empirical approximations must be recalculated for every new situation (Hamelers, 2004).

Deductive models use the laws of physics as a basis for a theoretical description of the process: they are mechanistic models. Few of them have been developed because of their complexity Hamelers (2004).

It is important to keep in mind that while models that do not fit the data are likely to be bad, one that does fit the data is not necessarily good (Hamelers, 2004).

The results of modelling in complex fields like environment and ecology are usually inadequate because the required parameters are not well-known. Hamelers (2004) gives a practical, deductive approach to compost modelling.

Most models use standard conservation equations, where $accumulation = inputs - outputs + transformation$ (Mason, 2006) and some models are based on deterministic equations, lumped parameters and stochastic models have been used (Mason, 2006; Seki, 2000).

2.3.4 Apparatus

Most published models represent in-vessel compost system, but windrows have sometimes also been modelled, including turning and shifting: at these times, simulations are paused and the parameters, such as temperature, are harmonized and redistributed according to certain rules (Bongochgetsakul and Ishida, 2008).

2.3.5 Spatial dependency

Spatial dependency exists in a compost reactor because the airflow, whether forced or natural, induces an asymmetry, heat is lost through the wall, and the compost itself compacts due to gravity. Not all models are highly resolved spatially. In his model Haug (1993) divided the reactor into 5 layers, and assumed homogeneity within each layer. Models like those of Petric and Selimbasic (2008); Sole-Mauri et al. (2007); Liang et al. (2004) have no or limited spatial dependency. Some of the recent models used Finite Element Methods to solve the partial differential equations with a high spatial resolution (Bongochgetsakul and Ishida, 2008). A more exhaustive list of these models can be found in Mason (2006).

2.3.6 Finite Element Method

As written in the Reference Guide of COMSOL^{TM1}, the Finite Element Method (FEM) approximates a system of partial differential equations (PDE) with a system that is a combination of elementary functions. These shape functions describe the possible forms of the approximate solution.

In order to solve the problem, this method decomposes the geometry into smaller shapes organized into a network called a mesh. The mesh can be 2D or 3D depending on the problem (Pepper and Heinrich, 1992). Usually triangles or pyramids are used for they are simply shaped, yet smoothly fit into larger, complex geometries.

The solution is then found by solving the equations for each element of the mesh, by a combination of simple interpolation functions, like the Lagrange polynomial. Continuity of the solution and its derivatives is required at the boundaries between the elements of the mesh.

2.4 Compost

2.4.1 Moisture content

Moisture content is one of the most important variables that needs to be controlled in order to have suitable conditions for microorganisms (Haug, 1993). The biomass lives within a water film, which is why completely dry compost will be inactive (Rynk, 1992). If water fills the pores of the compost, however, the diffusion of oxygen is impeded. In the areas far away from free air, oxygen will be depleted by the biomass faster than new oxygen can diffuse through the water. This scenario

¹ For more information about the software, see COMSOL AB (2008)

happens not only when the compost is completely saturated but even when water blocks key macro pores, while leaving bubbles of air imprisoned. The oxygen in these bubbles is soon depleted and their presence further slows the diffusion of oxygen.

The optimum moisture content has been discussed in many studies (Rynk, 1992; Jeris and Regan, 1973) and the reported results vary according to the compost mixture. Agnew and Leonard (2003) mention that the common best interval is around 50 to 60%, but that composting under higher or lower moisture conditions has been achieved (Uao et al., 1993).

According to Richard et al. (2002), a high moisture content can hinder biomass growth at an early stage, possibly be due to an adaptation time or to the low level of oxygen.

There is no clear relationship between optimum moisture content and the different stages of composting, but Richard et al. (2002) showed that the optimum is variable whether increasing or decreasing, during the early stages of composting.

Some studies have focused on matric potential instead of moisture content. Matric potential describes the binding force exerted by the porous media on the water, preventing its movement. The preferable range for the matric potential was found to be -10 to -20 *kPa* (Miller, 1989). The conversion between the optimal ranges of matric potential and moisture content must be made with care, since matric potential is a function of pore size distribution (Agnew and Leonard, 2003).

The moisture content can be reduced by air or heat drying, compaction or turning (Haug, 1993).

2.4.2 Residual water content

Residual volumetric water content or water retention characterizes the water left in a porous medium after a drying process. Due to surface tension, some water always remains, depending on the physical structure of the medium. Wallach et al. (1992) give some values for the residual water content for different kinds of compost, ranging from almost zero to 0.2, (unitless).

2.4.3 Bulk density

The bulk density of compost is a measure of the mass of material within a given volume (Agnew and Leonard, 2003). Bulk density can be evaluated for dry or, more commonly, for wet material. Dry and wet densities range, respectively, between 100 to 400 $kg\ m^{-3}$ and 500 to 900 $kg\ m^{-3}$ (Agnew and Leonard, 2003). The wet bulk density varies spatially as the material is denser at the bottom of the pile (Van Ginkel et al., 1999). Wet bulk density also changes with time as the compost compacts and the moisture content varies. The relation between moisture content and wet bulk density can be estimated with Eq. 3.17 according to Glancey and Hoffman (1994).

Values of dry bulk density for several types of compost were measured by Ahn et al. (2009).

Particle density is the most difficult of the fundamental properties to measure without special apparatus, but can be estimated from volatile solids and ash measurements, together with standard particle density values for these biochemical fractions (Richard et al., 2002).

2.4.4 Porosity

Porosity is the empty fraction of the volume of a porous material. By this definition, water-filled pores are also considered as void space. The free air space (FAS), however, is the air-filled fraction of pores (Haug, 1993). FAS is linked to moisture content by the relation $FAS = porosity - MC_{w.b.}$, where $MC_{w.b.}$ is the wet basis gravimetric moisture content. The porosity ranges, for the studies listed in Agnew and Leonard (2003), from 0.58 to 0.94. Porosity, and FAS more so, are important parameters to characterize the composting process as they are correlated to the circulation of air and the supply of oxygen. Some theory about air-filled porosity can be found in Richard et al. (2002) and typical values for several types of compost in Ahn et al. (2009).

2.4.5 Interactions

All of these parameters interact with each other, which makes the modelling problem even more complex. For instance, the bulk density varies with the water content, which has an impact on the air-filled porosity (Poulsen and Moldrup, 2007).

2.5 Biomass processes

2.5.1 Biomass population

Life in a compost mixture is diversified.

The bacteria are organisms living in compost and are mostly unicellular, although multicellular cooperation is common (Haug, 1993). Fungi are also important in the decomposition of substrate and can be separated into two types: mold and yeast. Molds are strictly aerobic while yeast can switch to anaerobic behavior when

the conditions require it. Fungi are larger and have more complex reproductive methods than bacteria, but they compete for the same resources. Descriptions of several species of each of these groups can be found in Haug (1993). The importance of bacteria was long neglected for fungi were easier to spot, but it has been shown that bacterial activity is important, especially at high temperatures (Diaz, 2007).

Different microorganisms do not necessarily feed on the same nutrients nor generate the same metabolites. Also the impact of pH, moisture content or temperature varies from one species to another. A common distinction is to separate microorganisms with regard to their dependency on temperature. It is known that some microorganisms' optimum temperature is around 30°C and that their growth is inhibited at higher temperatures: these are called mesophiles. The thermophiles grow at higher temperatures up to 60°C. It is unclear whether, in a composting mixture, strains of microorganisms can be clearly separated into those two distinct types or whether the optimum temperature for different strains of microbes follows a more continuous distribution.

In early models it was common to assume only one strain of microorganism in representation of the biomass (Stombaugh and Nokes, 1996). Implementing representation of different strains can be useful, however, in order to model different behaviors like mesophilic or thermophilic adaptation. It is also useful when trying to model the consumption of a substrate or the generation of a metabolite specific to a microbial strain, for instance, ammonia emission. Some models have included many different strains (Liang et al., 2004). Sole-Mauri et al. (2007) modelled six microbial

populations, each with a particular substrate specificity and optimum temperature for growth (with distinctive mesophiles and thermophiles).

Stombaugh and Nokes (1996) said that biomass activity concentrates first at the bottom of a vessel because of high temperature and reduced oxygen supply at the top.

2.5.2 Main equation

Biomass growth is typically modelled using Eq. 3.1, as in Stombaugh and Nokes (1996). Another way to model biomass growth is to focus on the substrate consumption, and to link this to biomass through a yield coefficient (Haug, 1993).

2.5.3 Impact functions

The impact of physical parameters on the biomass activity can be modelled different ways. Stombaugh and Nokes (1996) whose work is the basis for many models, linked physical parameters with the biomass growth through multiplicative impact functions. Others, like Richard et al. (2002) gave a relation between a normalized respiration rate (oxygen uptake) and parameter values. A third possibility is to link the decomposition rate of the substrate with these parameter values (Ekinci, 2004).

Temperature. As temperature increases, so does Brownian motion, which is fundamental to reaction kinetics, since particles interact only when they are in mutual contact. If there is more movement, then the contact happens more frequently, which speeds up the overall activity of microbes. This impact of temperature on growth is exponential (Haug, 1993). At higher temperatures, heat inactivation becomes more pronounced, however, so depending on the species of microorganism, the growth will rapidly decrease (Mayo, 1997).

Richard and Walker (2006) compared various correction functions for the effect of temperature on growth rate (Andrews and Kambhu, 1973; Ratkowsky et al., 1983; Rosso et al., 1993). The formula given in Rosso et al. (1993) has parameters with less variability over the course of the degradation process. In addition, the determination of parameters for this model is easier than for the others (Richard and Walker, 2006).

The following table shows three of the most used functions for implementing the impact of temperature on biomass growth. The plots of these functions can be seen in Fig. 2–1. The function used in Rosso et al. (1993) displays a shape that respects most of the required features as shown in Fig. 2–1 (b). This function, however, only illustrates the impact of temperature in the defined range: outside of its boundaries $[T_{min}; T_{max}]$ the function is not realistic. For instance, if the temperature goes beyond T_{max} the impact function becomes highly negative, see Fig. 2–1 (d). The two other functions do not present this drawback.

Table 2–1: Impact functions

Reference	Temperature function	See
Nielsen and Berthelsen	$\frac{\exp(a(T-T_0))}{1+\exp(b(T-T_1))}$	Fig. 2–1 (a)
Rosso et al.	$\frac{(T-T_{max})(T-T_{min})^2}{(T_{opt}-T_{min})((T_{opt}-T_{min})(T-T_{opt})-(T_{opt}-T_{max})(T_{opt}+T_{min}-2T))}$	Fig. 2–1 (b,d)
Stombaugh and Nokes	$\begin{cases} \frac{T}{T_2-T_1} & T_1 \leq T < T_2 \\ 1 & T_2 \leq T < T_3 \\ \frac{75-T}{75-T_3} & T_3 \leq T \end{cases}$	Fig. 2–1 (c)

Whereas many studies used piecewise and other empirical functions (Stombaugh and Nokes, 1996; Liang et al., 2004), deductive functions were also used, based on Arrhenius’ law (Bongochgetsakul and Ishida, 2008; Nielsen and Berthelsen, 2002).

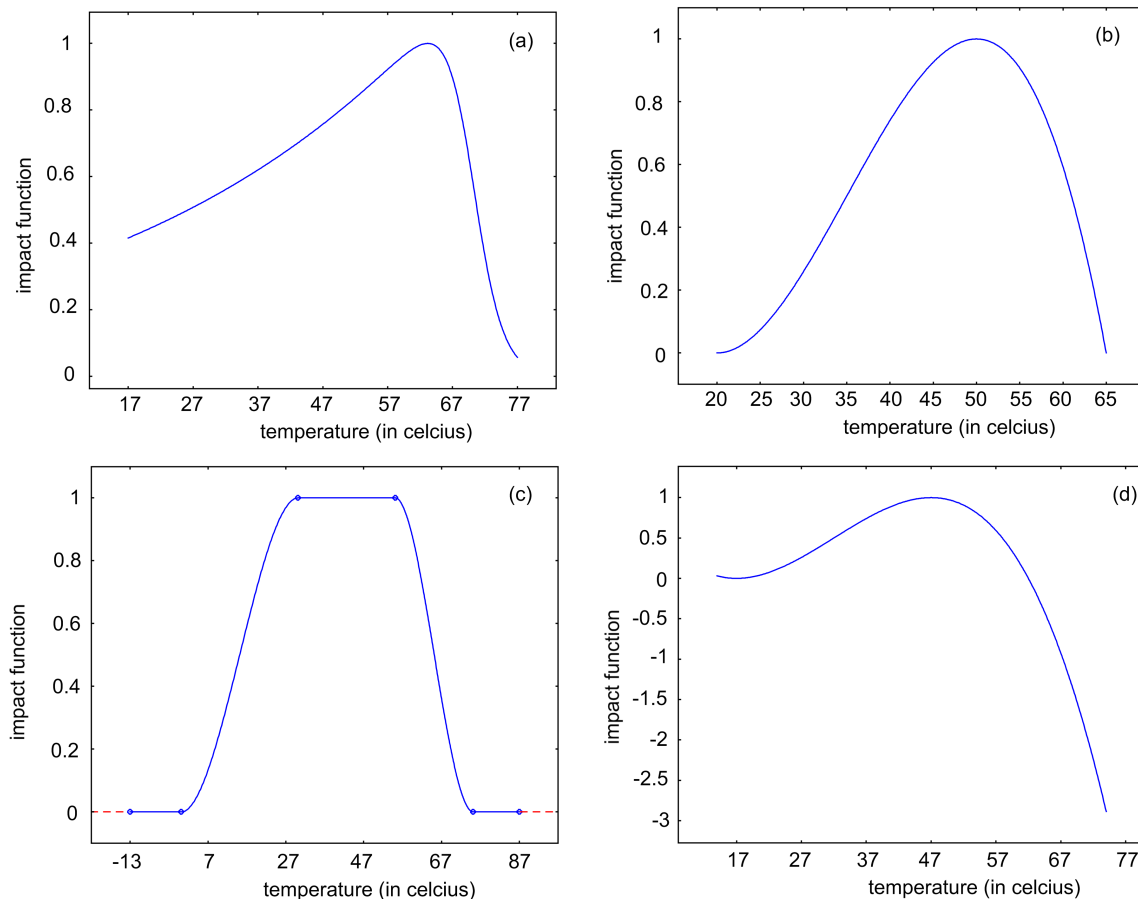


Figure 2-1: Impact functions of temperature used by Nielsen and Berthelsen (2002) (a), Stombaugh and Nokes (1996) (c), and Rosso et al. (1993) (b and d for different ranges of temperature).

Moisture content. Moisture content is critical for all living organisms and microorganisms likewise need water to grow and move. Microorganisms require water for the transportation of nutrients: their growth is inhibited when the amount of water is not sufficient (Miller, 1989). Below 20% moisture, biomass activity ceases (Haug, 1993). At high moisture content, the FAS is so reduced that the

supply of oxygen is inadequate for biomass activity. This effect is accounted for in the impact function of moisture content by decreasing the value of the function when the moisture content is close to 1.

Oxygen availability. Oxygen is a critical parameter for biomass as it is required to produce ATP, which is the molecule that stores energy for the whole cell. Without oxygen, the biomass, which is assumed to be aerobic, does not grow. The growth rate increases rapidly with oxygen concentration up to a maximum growth rate beyond which additional oxygen makes no difference. Following the work of Stombaugh and Nokes (1996), the most common impact function used is a Monod function (Eq. 3.5). The only constant in this equation is the half-velocity rate, which represents the amount of oxygen at which the growth rate is half its maximum value.

The biomass absorbs oxygen from the liquid phase, so the half-velocity rate should be expressed in terms of concentration of dissolved oxygen. Because of the equilibrium between oxygen in the liquid and gas phases, however, the half-velocity rate is often expressed as the concentration of oxygen in the gas phase (Stombaugh and Nokes, 1996). The gaseous oxygen concentration is useful in models in which the liquid phase is not explicitly represented.

Mason (2006) cites studies in which the half-velocity constant of the Monod equation was formulated as dependent on temperature and moisture content, which improved the accuracy of the models.

Substrate availability. The substrate is the nutrient source of the biomass and thus is necessary for its growth. A Monod function is often used to model the substrate availability impact on the biomass growth rate.

pH. The optimum pH for microbes is between 5.5 and 8: while a neutral pH is better for bacteria, fungi prefer a slightly acid one (Diaz, 2007). The pH impact function decreases when the pH moves away from the optimum value (Mayo, 1997).

2.5.4 The impact of biomass on other variables

Just as physical properties impact the biomass activity, the latter also affects many physical properties.

Microbial degradation of substrate is exothermic. Mason (2006) reported that heat conversion factors range from 17.8 to 24.7 $kJ g^{-1}$ as normalized with respect to the disappearance of volatile solids, or from 9760 to 14000 $kJ g^{-1}$ with respect to oxygen consumption. Those figures are based on the general stoichiometry of the combustion of substrate (Bongochgetsakul and Ishida, 2008; Petric and Selimbasic, 2008). Thanks to these relationships, the amount of oxygen or substrate consumed can be used to predict how much carbon dioxide, water vapor, or ammonia is released (Petric and Selimbasic, 2008). As stated by Mason (2006), water produced by the metabolic activity of the biomass, as well as the oxygen consumed and the carbon dioxide released, have only been modelled using a yield coefficient.

2.6 The substrate

Most compost material comes from plants, while animal tissue and microbial biomass represent only a small fraction of the overall mass, although these are usually the most nutrient-rich fraction (Diaz, 2007).

The main natural compounds in compost are lignin and cellulose or, more generally, glucose polymers. Lignin is a major structural component of plants and is hard to decompose. Usually these compounds are degraded by fungi in low yield reactions (Diaz, 2007).

The carbon to nitrogen ratio of compost is an important predictor of the growth of the biomass and is also an indicator of the maturity of compost. This ratio is often taken into account in mathematical models (Liang et al., 2004; Sole-Mauri et al., 2007). This ratio usually decreases during composting (Diaz, 2007). A starting C:N ratio of 25-30 is optimal according to Diaz (2007), who also reported the value of the ratio for several organic wastes.

2.6.1 Main equation

The degradation of the substrate is mediated by the existing biomass, for self-maintenance and by the growth of new biomass. The equation used by Stombaugh and Nokes (1996) is that which is the most commonly used (Eq. 3.8).

2.6.2 Different types of substrate

The substrate can be partitioned into different fractions such as, for instance, soluble or insoluble compounds (Lin et al., 2007). Usually, sources of carbon and nitrogen are represented separately. The easiest way to partition the substrate, however, is to match the components as nutrient sources for different strains of microorganisms. In Sole-Mauri et al. (2007), five different substrate categories were implemented: carbohydrates, proteins, lipids, hemicelluloses, and lignin. The effect of different C:N ratios on the initial growth rate was also modelled.

In the situation where several kinds of substrate are modelled (Sole-Mauri et al., 2007; Lin et al., 2007), each is represented by the same general equation, but with specific coefficient values.

2.7 Physical processes

2.7.1 Porous media

Tortuosity. The tortuosity accounts for the complexity of paths in a porous medium, and is defined as the square of the ratio of the effective path length to the straight distance between two points in the compost bed (Grathwohl, 1998). The capillary model represents a porous medium as a set of parallel, straight pores, whereas it is actually a maze where the path are longer. The tortuosity compensates for this approximation by increasing the length of the parallel straight pores (Epstein, 1989). The definition of tortuosity is only significant in a medium where the pore sizes are homogeneous (Grathwohl, 1998). According to Dykhuizen and Casey (1989) a homogeneous, isotropic porous medium has a tortuosity factor of 3. Practically, however, the determination of this coefficient is difficult and tortuosity is often used as a “fudge factor” (Grathwohl, 1998).

2.7.2 Fluid dynamics

The flow of gas removes vapor and heat, and is fundamental to any model of composting processes. Some models represent only one inlet and one outlet and neglect the fluid dynamics within the reactor (Petric and Selimbasic, 2008; Sole-Mauri et al., 2007; Liang et al., 2004). Stombaugh and Nokes (1996) explicitly modelled the movement of air between each of the 5 layers in their model but did not specify the fluid dynamics.

When they are modelled the fluid dynamics are usually described by the Navier-Stokes equations in COMSOL AB (2008).

At low airflow rates, oxygen is rapidly depleted, and the high temperature inhibits the biomass growth. High aeration rates lead to faster substrate consumption and microbial growth, but also cause faster drying (Stombaugh and Nokes, 1996).

The values of the coefficients describing airflow in porous media are well-known. The dynamic viscosity of air is dependent on temperature (Montgomery, 1947). Permeability of the compost to air (Van Ginkel et al., 2002) is described as a function of bulk density and volumetric water content, or the gas-filled, fraction using Darcy's law (Poulsen and Moldrup, 2007; Van Ginkel et al., 2002).

Relation between pressure drop and airflow. Darcy's law links the air velocity and the difference in pressure. For a porous medium, however, the relation and coefficients need to be modified. Several studies have focused on this relationship (Miller, 1989; Saint-Joly et al., 1989; Stombaugh and Nokes, 1996; Poulsen and Moldrup, 2007). According to Agnew and Leonard (2003) the relation between airflow and pressure drop used in several studies (Keener et al., 1993; Mu and Leonard, 1999; Saint-Joly et al., 1989) was $\Delta P = aV^n$, where ΔP is the pressure gradient ($mm H_2O$), V is the airflow ($m^3 day^{-1}$), a and n are parameters which range respectively from 1.17 to 2.02 and 1.62×10^{-5} to 2.69×10^{-7} . Airflow is also influenced by compaction. Mu and Leonard (1999) mentioned that during their experiments, the compost settled by about 10% of its original depth and the flow resistance increased substantially.

2.7.3 Heat transfer equations

The heat generated by the biomass is transferred by convection and conduction in both the liquid and gas phases. Some heat will be lost through the walls of the compost vessel while the majority will be expelled at the outlet with the exhaust air.

Heat transfer model. The heat generated by the biomass and the latent heat of evaporation are the most important terms in the heat transfer equations (Mason, 2006). Mason (2006) listed articles in which conductive heat loss through the wall was modelled with an overall heat transfer coefficient. Radiative heat loss is almost never taken into account, although, according to Robinson et al. (2000), it is significant in open windrows. Haug (1993) also mentioned that, during turning, there is a rapid surface temperature drop due to radiative and convective heat loss.

Many studies were based on enthalpy balances, as shown in Stombaugh and Nokes (1996); Liang et al. (2004) and Sole-Mauri et al. (2007). Some more complex equations have also been used that couple heat and water transfer using the matrix potential (Bongochgetsakul and Ishida, 2008).

Thermal properties of compost. During composting, the composition of the substrate changes as it is degraded. Furthermore, the moisture content also varies. Thermal properties of compost also vary as a result. Keener et al. (1993) used the formula $C_{compost} = 1.48 - 0.64 ASH + 4.18 MC_{d.b.}$, where $C_{compost}$ is the heat capacity of compost ($J kg^{-1} K^{-1}$), ASH is the mineral content, and $MC_{d.b.}$ is the dry basis gravimetric moisture content. Ahn et al. (2009) reported values of thermic coefficients, and their dependency with temperature, water content, and different

kinds of compost. Van Ginkel et al. (2002) also showed that thermal conductivity increased with temperature.

Thermal properties of compost are difficult to measure because compost is a heterogeneous medium, being composed of air, water, and dry matter. Even the dry matter is often heterogeneous in the case of mixed compost. Chandrakanthi et al. (2005) experimented with methods to integrate the thermal conductivity of these three phases of the substrate to find the overall thermal conductivity of compost.

2.7.4 Diffusion

Diffusion is mass transport due to the thermal motion of molecules by a random process known as Brownian motion (Grathwohl, 1998). There are two common models of diffusion (Cussler, 1997): in the first it is assumed that flux is proportional to a difference in concentration, as modulated according to a mass transfer coefficient. In the second it is assumed that increasing the capillary length decreases the flux as modulated according to a diffusion coefficient. The latter is often called Fick's law. Neither of these two models is always accurate because of their intrinsic assumptions: for instance, the flux may not be proportional to the difference in concentration if the capillary is very thin or if there are reactive compounds involved (Cussler, 1997). Fick's law is the most general and fundamental model, but in some cases the situation requires a more phenomenological approach and the mass transfer model may be more accurate (Cussler, 1997).

The value of the diffusion coefficient depends on the mass and the ionic radius of the diffusing molecules, temperature, and the medium through which diffusion occurs (Grathwohl, 1998).

In porous media, diffusion can be hindered by the tortuous paths that the molecules must follow, and the small cross-sectional areas of the channels that they must traverse if the pore size is small (Grathwohl, 1998). The movement of molecules, in addition to the random nature of Brownian motion, is also influenced by these factors. It is possible, however, to use Fick's law by substituting an effective diffusion coefficient that takes into account these parameters.

The diffusion of dilute molecules into the aqueous phase of a water-saturated porous medium is still dominated by intermolecular collisions, as long as the mean free path of the molecules is smaller than the average diameter of the pores (Grathwohl, 1998). In other circumstances, the use of Knudsen's theory of diffusion is more appropriate. Measurements of diffusion coefficients are hard to obtain, but some predictive equations have been formulated (Grathwohl, 1998).

2.7.5 Mass transfer across interfaces

Mass transfer across an interface cannot be well modelled with equations like $\text{flux} = \text{mass transfer coefficient} \times \Delta \text{ concentrations}$. The reason is that the concentration of a solute is not constant nor independent of the distance from the boundary. One way to tackle this problem is to assume that a stagnant film, or boundary layer, exists near every interface. This approach, first introduced by Walther Nernst in 1904, neglects convection near the boundary. Two diffusive processes are considered: one from the bulk fluid to the boundary layer and the other through the boundary (Cussler, 1997). More details can be found in the methodology.

Cussler (1997) mentions other theories that have been developed more recently, like the penetration theory (Higbie, 1935), the surface renewal theory (Danckwerts, 1951), and Graetz-Nusselt boundary layer theory (Levich and Spalding, 1962).

2.7.6 Water equations

In the air, water vapor is carried by the airflow so that its movement is a regular problem of convection and diffusion. The water movement in the liquid phase is not as easy to model. Compost is a porous medium, so capillary forces and surface tension prevent the liquid from moving so easily.

Diffusion in porous media depends on the amount of water present and its matric potential. Matric potential and moisture content are linked (Miller, 1989; Parr et al., 1981). Matric potential describes the force with which water is held within capillaries and on surfaces, and it is related to the radii of the water-filled capillaries. In soil systems, matric potentials from 0 to - 15 kPa have been associated with oxygen limitation.

Mathematical relations between soil water retention and pressure head have been proposed by van Genuchten (1980), who also described the hydraulic conductivity and diffusivity as a function of the normalized water content. Those relations work best at low to medium water content, as soil diffusivity reaches infinity when the moisture content approaches to the saturated value. At that point the equations need to be redefined. Values for the water diffusion coefficient can be found for several kind of compost in Wallach et al. (1992). Many models were implemented following a simpler approach for the diffusive transport of moisture (Mason, 2006).

Conversely, the diffusivity of substrate in water and its relation to water content ($D = k \times \text{water content}^3$) are tackled in Parr et al. (1981).

Bongochgetsakul and Ishida (2008) distinguished between the liquid and gas phases but integrated both of the terms into the same PDE.

As for the gas phase, Montgomery (1947) studied the dependency of the diffusivity of water vapor with regard to temperature.

The equilibrium between the water in the liquid and gas phases, as well as the kinetics of the water mass transfer, were developed in Petric and Selimbasic (2008) by using psychrometrics.

2.7.7 Oxygen equations

The movement of oxygen in the air occurs by convection and diffusion. In the liquid phase, the depletion of oxygen due to biomass respiration is compensated by diffusion through the liquid-gas interface.

The diffusion of gas in the water and gas phase of a porous medium were studied by Tse and Sandall (1979) and Van Ginkel et al. (2002).

The mass transfer of oxygen through the boundary layer follows Henry's law (Petric and Selimbasic, 2008). The same authors also gives a description of the kinetic of mass transfer through the interface.

2.8 Other processes

Many other processes were not included in this model, for instance the production of ammonia (Liang et al., 2004) or carbon dioxide. Those two effects are often modelled as linear functions of the biomass activity.

2.9 Sensitivity

Sensitivity analysis is the study of the response of an output to a set of perturbations in the input. It may be useful in many ways. For systems that need to be strictly controlled, like a nuclear plant, sensitivity analysis is needed to determine the parameters that have the most significant impact on the system. The experimenter can then focus on controlling those specific factors. Sensitivity analysis can be used when developing models of complex systems to determine which inputs have insignificant effects. Those inputs can be considered as constant, thus simplifying the model. In situations where limited resources are available to acquire input data, sensitivity analysis can help to determine which inputs should be emphasized, i.e. those inputs to which the model response is the more sensitive.

Sensitivity analysis is comprised of stochastic and deterministic methods. Reviews can be found that list many of them, as well as explain their advantages and drawbacks (Hamby, 1994; Frey and Patil, 2002). Several coefficients have been defined that characterize the sensitivity of a model (Hamby, 1994), such as the Pearson number. Instead of indicating the most sensitive parameters, those numbers evaluate how sensitive the model is to generic perturbations.

2.9.1 Stochastic methods

Stochastic methods focus on the distribution of values of the model's output variables to a random sampling of input variables. This method is efficient when simulations run quickly, because many simulations are usually required in order for the statistics to be significant.

2.9.2 Deterministic methods

Deterministic methods can only be used if the model itself is deterministic. Sometimes these methods are used to identify key parameters, the sensitivity of which is then studied with stochastic methods. The simplest method is to fix the values of all the parameters but one, then vary the values of that parameter around its standard value. More elaborate techniques have, however, also been devised.

The differential method is one of the most common methods of differential sensitivity analysis (Hamby, 1994) and is basically a first-order Taylor series approximation of the dependent variable, the output, as a function of the independent variables, the inputs (Chang and Wen, 1968). This method and its variants are computationally efficient but require the solution of the model equations, which may be difficult or impossible. When the dependent parameter cannot be described algebraically, an approximation of the partial derivatives can be made through finite differences (Gardner and O'Neill, 1981). These methods can be easily implemented with matrices, which makes them suitable for computational applications.

2.9.3 Sensitivity of compost models

Complex sensitivity methods have been used in many fields (Lamboni et al., 2009; Kucherenko et al., 2008; Crestaux et al., 2008). In composting, however, sensitivity studies were usually done by varying a single parameter from its original value and plotting the results of the output. The magnitude of the variations was usually based on a percentage of the initial value; the common percentages used were -75%, -50%, -25%, +25%, +50%, +75% (Liang et al., 2004; Petric and Selimbasic, 2008; Sole-Mauri et al., 2007; Stombaugh and Nokes, 1996). These analyses were focused

on outputs like the peak ammonia emission, the peak temperature, etc. The airflow and microbial growth rate have been shown to have a great impact on those outputs.

CHAPTER 3 Methodology

3.1 Description of mathematical modelling

The overall objective of this study was to model and understand the composting process, ultimately to help managers to obtain good quality compost as quickly as possible. The compost quality is heavily dependent on the relative proportions of basic nutrients like carbon, and nitrogen. Changes in these nutrient concentrations are monitored during the simulation to track the overall quality of the compost. It is not possible, however, to model the evolution of only a few parameters without modelling the whole system.

As many studies have already shown, adequate provision of oxygen is necessary to meet these goals. This model includes both forced and passive aeration – through buoyancy forces – but simulations were focused on forced aeration, for passive aeration can be considered as an extreme case of forced aeration in which the forced component is negligible. Passive aeration can play an important role even in systems that are actively aerated.

The aerobic decomposition of nutrients is of greater importance than the anaerobic, for the reaction is faster and produces far less noxious or environmentally harmful gas. In industrial and research composting, therefore, the intention is that processes be aerobic.

The key objectives of this project were:

- combine elements of models published in the literature to create an integrated model;
- model the most important features mentioned in the literature with a high spatial resolution;
- design a user-friendly model that is easy to modify;
- create a model that can be easily used for optimization of composting processes.

3.2 Geometry

Composting usually happens in piles, windrows, or vessels. The most convenient apparatus for use in a lab is the vessel, for reasons of practicality; for instance, the inlet and outlet gas can be monitored more efficiently. This is why in-vessel composting is more commonly reported in the literature. This model could be further developed for validation against experimental data, so the geometry was chosen to represent a vessel.

The model was used in simulations to describe composting in a long rectangular channel. A vertical slice is shown in Fig. 3–1. We assumed that the vessel was long enough that the effects of the extremities of the vessel, especially heat loss, could be neglected. This geometry approximates that of the channel composters found in many large-scale facilities.

The circulation of air was implemented by introducing inlet ducts at the bottom of the barrel and exit ducts at the top, where the air exited unimpeded. This configuration was chosen so that the airflow circulated in the same direction as the passive aeration, due to heating within the compost. A fan provided a constant

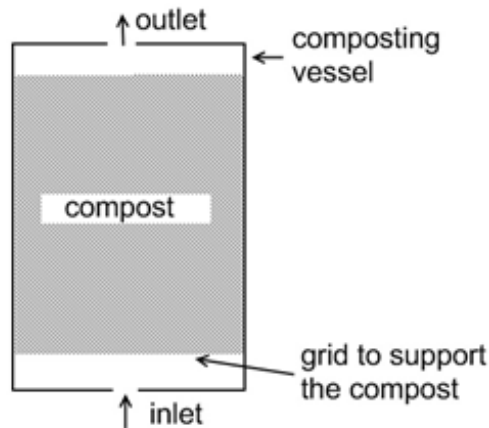


Figure 3–1: Schematic of a closed composting vessel. The compost is represented by the shaded area. It is supported by a mesh that is fine enough to prevent the compost from falling, yet coarse enough to let the air pass through. Fresh air is supplied through the inlet duct vent and exhausted through the lid.

pressure drop at the inlet. Ambient air was blown in through the bottom. A mesh supported the compost to create an aeration plenum extending several centimeters above the inlet duct in order to uniformly distribute the inlet air. In the model it was assumed that a constant and homogeneous air flow was blown from the bottom of the rectangle. The vessel prevented any entry or exit of gases other than through the aforementioned vents.

The compost within the barrel was assumed to remain static, and was not turned or changed during the simulation. As the vertical air flow and the horizontal loss of heat through the sides of the vessel suggest, however, spatial variability will arise even with initially homogeneous compost. This model had high spatial resolution in order to follow the development of such variability.

The study of this variation gave another perspective to the interpretation of composting process. It was also interesting to see whether the geometry of the vessel had an impact on different aspects of composting like the time of peak temperature, or the total substrate degraded.

3.3 The solver

The finite element methods already implemented in COMSOL AB (2008) were used to solve the partial differential equations of the model. COMSOLTM has built-in sets of common equations that were used in this model: the convection and conduction module for heat transfer, the fluid dynamic module, the convection and diffusion module for mass transfer, and the diffusion module were used. Also, COMSOLTM allows the user to implement his own PDEs through a “PDE general form” module.

The mesh was designed using the default mesh algorithm in COMSOL AB (2008).

The analysis was made using the transient type (time-dependent) solver. A linear approximation was used with the Direct (UMPFPAK) method. The relative and absolute tolerance were respectively set to 0.01 and 0.001.

3.4 The compost

3.4.1 Overview

Composting is the stabilization of organic waste, ranging from cut grass to manure, to food waste. The characteristic size of compost particles ranges from 0.1 mm to several centimeters. Because of this aggregate structure, compost is a porous medium. The distribution of material in compost is not homogeneous. Two

factors make it complicated, however, to take into consideration the heterogeneity of the compost. The first is that it is impossible to know the complete distribution of particles, aggregates, and pore spaces in an actual compost pile. It would also be impossible to implement such an elaborate spatial model, let alone simulate the development of complex processes on such a geometry. Thus, the composting matrix is usually assumed to be homogeneous, and has been modelled in terms of mean values. For example, the substrate bulk density takes into account the porosity.

3.4.2 A three-phase system

Compost is a three-phase system. The organic solid phase is slowly dissolved in the water film that surrounds it. All the biomass activity is presumed to happen in this liquid phase. Microorganisms consume dissolved substrate and oxygen to grow, originating from the gas phase that circulates within the pores. This kind of geometry can be seen in Fig. 3-2.

3.4.3 A porous medium

The physics of a porous medium is characterized by several parameters, one of which is the porosity, which is the ratio of void space to the bulk volume of material. The permeability of a porous media quantifies its ability to transmit fluid. The constrictivity is related to the ratio of the diameter of the diffusing particle to the pore size. It is a scaling parameter which characterizes the fact that the diffusive flow is lower close to the walls. So, the less space there is between the walls, the slower the flow. Tortuosity is an evaluation of the complexity of the network of pores. The tortuosity is assessed by looking at all the pathways from one side to the other of the porous medium. The tortuosity of each pathway is the ratio between its total length

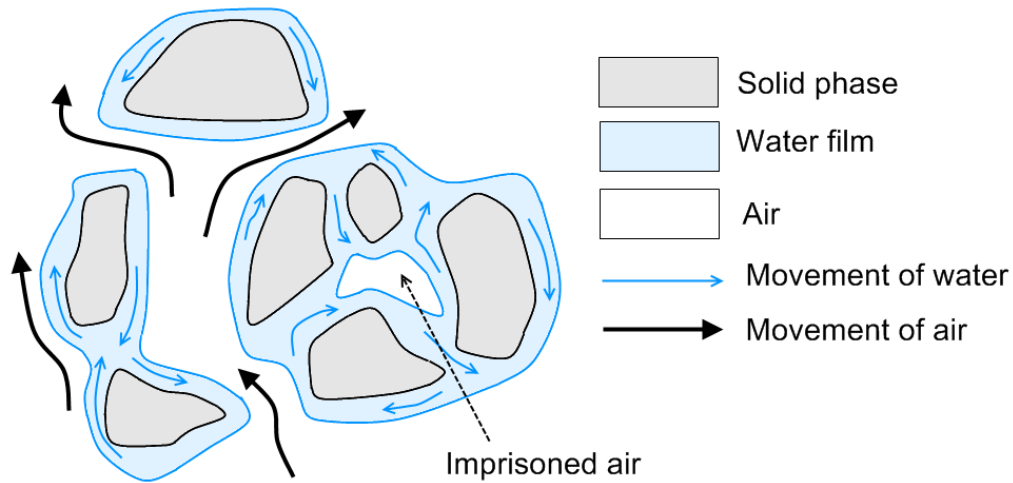


Figure 3-2: Schematic of a porous medium. The solid particles are covered by a water film. Depending on the moisture content, some empty pore space will be left for the air to circulate.

and the direct distance between the starting and ending points; hence it is always higher than 1, and a straight pathway has a tortuosity of 1.

3.5 The biomass

3.5.1 Main equation

This model was centered on the growth of microbial biomass. It is commonly assumed that the growth of biomass can be modelled by an exponential expression. The explanation is that, on average, a microorganism is assumed to have μ offspring during a unit of time, hence:

$$\frac{dX}{dt} = (\mu - k_d)X \quad (3.1)$$

Where X is the amount of biomass per units of volume ($kgX m^{-3}$), μ is its growth factor (s^{-1}), and k_d stands for the proportion of death within the population per unit of time (s^{-1}).

Initial conditions. The biomass was assumed to be uniformly distributed, with a density of X_0 .

Boundary conditions. The flux of the biomass at the boundaries was zero, because there was no loss nor addition of compost through the walls.

3.5.2 Impact functions

This equation is fairly straightforward in the case where k_d and μ are constant. If the death rate is assumed to be constant, as is often the case, then the growth rate depends on several parameters like temperature, oxygen content, humidity, and substrate nutrient concentration. The impact of those parameters is often modelled as a multiplicative product. Thus,

$$\mu = \mu_{max} \cdot f_{O_{2dis}}(O_{2dis}) \cdot f_T(T) \cdot f_{H_2O_{liq}}(MC_{w.b.}) \cdot f_S(S) \quad (3.2)$$

... where $f_{O_{2dis}}$, f_T , $f_{H_2O_{liq}}$, and f_S are dimensionless functions with values ranging from 0 to 1 and which represent the impacts of oxygen, temperature, moisture content, and substrate on the growth of microbial biomass (Stombaugh and Nokes, 1996). The closer the value of these functions to 0 the less positive is the influence of the parameter on growth. During the composting process, the value of μ reached different values depending on the time and location. The value of μ was high during the early stage, however, when there was no limiting factor other than the biomass concentration itself.

The impact of temperature. Experiments in the literature usually showed that temperature inside the compost quickly increased before it slowed or stagnated at a plateau at about 40°C. The temperature then rose again up to about 70°C, at which point the growth was totally inhibited. The reason for the plateau has not been determined. One explanation assumes the division of the biomass into types with different metabolisms. The biomass is often modelled as being composed of two general kinds of microbes: mesophilic and thermophilic. The mesophiles dominate at temperatures from 25 to 40°C. Those microorganisms are more sensitive to heat, however, than the thermophiles, and stop growing after 40°C. At higher temperatures, thermophilic organisms are responsible for the degradation. The plateau is explained because at 40°C, the thermophilic biomass is still small while the mesophilic has stopped growing. Thus the temperature stops increasing and needs the thermophilic biomass to start growing before it can rise again. This theory has yet to be tested.

The spatial dependency that COMSOLTM offers might give information on this subject as it is able to model biomass and temperature distribution at any place in the compost over time. An easy way to test the two-metabolisms theory would be to implement two strains of microorganisms with different of response curves for temperature, and to divide the biomass accordingly.

The impact function f_T can be modelled by:

$$f_T(T) = \frac{A_T e^{-\frac{E_1}{RT}}}{1 + K_T e^{-\frac{E_2}{RT}}} \quad (3.3)$$

... and is a modified version of the Arrhenius equation, to take into account the activity of the enzymes that moderate the microorganisms' growth (Nielsen and Berthelsen, 2002). In this expression, T is the temperature of the compost (K) and R is the ideal gas constant ($J K^{-1} mol^{-1}$). E_1 and E_2 are the energies of activation and inhibition of one strain of bacteria ($J mol^{-1}$), and differ between mesophiles and thermophiles. A_T and K_T are two dimensionless constants.

This equation takes into account two phenomena: the first is that the activity of enzymes – and more generally, of the microorganisms – increases with temperature. This is due to the fact that higher temperature means higher Brownian movement, and it increases the probability of an enzyme meeting its reagents. The second is that, at extreme temperatures the spatial configuration of enzymes is altered and their activity within the bacteria is prevented.

This equation, however, is hard to use because the coefficients are large – about 10^{40} . In order to avoid the huge difference in the order of magnitude between coefficients, a Taylor series expansion can be performed. The result is the following impact function according to Nielsen and Berthelsen (2002).

$$f_T(T) = \frac{Ae^{a(T-T_0)}}{1 + e^{b(T-T_1)}} \quad (3.4)$$

... where a and b are coefficients given by Nielsen and Berthelsen (2002). A is a scaling coefficient that ensures the function stays between 0 and 1. T_0 is an arbitrary temperature constant with a value determined for accuracy (Nielsen and Berthelsen, 2002). T_1 is the temperature that is at the inflection point, around $4^\circ C$ below the maximum temperature.

The impact of oxygen. The microorganisms were assumed to be aerobic. It has been shown that biomass activity is highly dependent on oxygen concentrations when the latter is low. When the oxygen content is higher than a specific threshold, however, its influence on the growth of the microorganisms plateaus. The impact of the oxygen content on the growth of the biomass was represented with a Monod function (Stombaugh and Nokes, 1996).

$$f_{O_{2dis}}(O_{2dis}) = \frac{O_{2dis}}{K_{O_2} + O_{2dis}} \quad (3.5)$$

... where O_{2dis} is the concentration of dissolved oxygen in the liquid phase ($mol\ m^{-3}$) and K_{O_2} is the half-velocity constant for oxygen ($mol\ m^{-3}$), i.e. the amount of oxygen required to reach half the optimum rate: $f_{O_{2dis}}(O_{2dis} = K_{O_2}) = \frac{1}{2}$.

This half-velocity constant can be evaluated with regard to the concentration of oxygen in the air (Stombaugh and Nokes, 1996). The concentration that is really important, however, is the one in the water film, as it is the only oxygen that is accessible to the biomass. The value given by Stombaugh and Nokes (1996) must be adapted in order to obtain the right K_{O_2} for the liquid concentration. The new value was computed using Henry's law for the equilibrium state: when $O_{2ex} = 0$ in Eq. 3.37.

The impact of substrate. The impact of the substrate availability was assumed to have the same form as that of oxygen (Stombaugh and Nokes, 1996), hence the function:

$$f_S = \frac{S}{K_S + S} \quad (3.6)$$

Here, S is the amount of substrate per unit of volume ($kgS m^{-3}$), K_S is the half-rate velocity constant for the substrate ($kgS m^{-3}$): the amount of substrate that reduces the maximum growth rate by half. This relationship represents the fact that, below an amount of substrate of K_S , the scarcity of substrate makes it difficult for the biomass to grow.

The impact of moisture content. As the biomass grows within the water film, the water availability determines the volume in which the microbial activity will take place. Thus, increasing the water content improves the growth capacity of the biomass by decreasing the effect of overpopulation: the less the competition for space, the higher the diffusion of nutrients. The thickness of the water film, however, increases with the water content. The thickness of the water film decreases the diffusion of the dissolved oxygen and slows the growth of the biomass. The impact function of the water content on the growth of the biomass must reflect both of these effects. The function chosen was that proposed by Smith and Eilers (1980). In this definition, $MC_{w.b.}$ is the moisture content (0 to 1):

$$f_{H_2O_{liq}}(MC_{w.b.}) = \exp(-10.973(0.7 - MC_{w.b.})^2) \quad (3.7)$$

The moisture content is defined as $MC_{w.b.} = \frac{O_{2dis}}{O_{2dis}+S+C_{NVS}}$ and is the ratio of the mass of liquid water in the compost to the total mass of compost. C_{NVS} is the non-volatile solids concentration ($kg m^{-3}$), which is the mass of matter that cannot be consumed by the biomass.

3.6 The substrate

3.6.1 Main equation

The substrate was reduced by the microbial biomass in two ways, as described by:

$$\frac{dS}{dt} = \min\left(\frac{dX}{dt}, 0\right) - \eta_{max} \cdot f_{O_2dis}(O_{2dis}) \cdot f_T(T) \cdot f_{H_2Oliq}(MC_{w.b.}) \cdot f_S(S) \cdot X \quad (3.8)$$

... where S and X are the amount of substrate and biomass per unit of volume respectively.

The first term represents the consumption of substrate required for the increase of the biomass due to its growth: $Y_{X \rightarrow S}$ is the yield coefficient of the creation of biomass ($kgX kgS^{-1}$) and its value is negative. This term only exists when the mass of microorganisms is increasing, hence the minimum value of zero. The second term stands for the uptake of the existing biomass to sustain itself, η_{max} being the maximum microbial maintenance coefficient ($kgS kgX^{-1} s^{-1}$) (Stombaugh and Nokes, 1996).

There are other possibilities to model the change in the substrate mass. The uptake of substrate by the biomass can be implemented as proportional to the oxygen consumption. This approach is interesting because the stoichiometry of oxygen consumption in the biomass growth is assumed to be constant. One problem of this approach is that the oxygen is mathematically deduced from the biomass growth.

The presence of an intermediary increases the possibilities for error and imprecision. Equation Eq. 3.8 was chosen because it is directly dependent on the biomass, although there are still some inaccuracies when the growth rate is very small.

3.6.2 Initial conditions

The substrate was assumed to be uniformly distributed, with a density of S_0 .

3.6.3 Boundary conditions

The flux of substrate at the boundaries was assumed to be null for the same reason as for the biomass.

3.7 Physical processes

3.7.1 Main equation

Compost is a three-phase system. The solid phase, the organic waste, is slowly dissolved in the water film that surrounds it. In this model, all the biomass activity was presumed to happen in this liquid phase. Microorganisms consume dissolved substrate and oxygen to grow. The growth of biomass releases water and heat as by-products. Heat and water are exchanged from the water film at the interface with the gas phase. The gas is continuously replaced by fresh air through the ventilation system. Here, it was assumed that all the nutrients in the substrate were readily dissolved and available to the biomass, so the focus was on the liquid and gas phases.

In order to adequately model the physical properties of compost, one needs to model both the liquid and gas phases. The evolution of the biomass happens over weeks, whereas physical processes like heat and mass transfer in air happen within hours, so using pseudo-stationary solutions for the physical equations is a common

way to simplify the problem. In this work, however, all the physical processes were solved under transient conditions.

3.7.2 Diffusion in porous media

Diffusion is a dominant process in composting. Diffusion laws are not the same, however, in porous media as in a free space. Thus Fick's second law $\frac{d\phi}{dt} = D\Delta\phi$, where ϕ is the concentration ($mol\ m^{-3}$) and D the diffusion coefficient ($m^2\ s^{-1}$), cannot be used directly. The physics of diffusion in porous media depends greatly on the typical size of the pores.

Gas particles in a free zone will move erratically following Brownian motion: they will go straight in one direction until they hit another particle that will alter their path and make them head in another direction. In restricted areas, however, particles tend to rebound from the wall more often than with other particles, and their movements follow a different pattern. This behavior happens when the characteristic dimension of the space is smaller than the mean free path of a particle, which is the average distance covered by a particle between two impacts. A theoretical model of this pattern of movement is called Knudsen diffusion. The formula for the mean free path l is

$$l = \frac{k_B T}{\sqrt{2}\pi d^2 P}$$

...where k_B is Boltzmann's constant ($J\ K^{-1}$), T is the temperature (K), d the diameter of the particle (m) and P the pressure (Pa). For ambient conditions, l is between 10 and 100 nanometers, which is much smaller than the size of macro pores in compost media. Pores of that magnitude do exist in compost, but the physics of the system – i.e. the fluid dynamics, the exchanges at the liquid/gas interface, etc –

will be dominated by the bigger pores. Knudsen diffusion theory, therefore, was not used in this model and a continuous model was selected instead.

Fick's second law was used to model diffusion within the compost, but with an effective diffusion coefficient that took into account the specific properties of porous media (Cussler, 1997). The effective diffusion coefficient was derived from the regular diffusion coefficient by the formula: $D_e = \frac{D\epsilon_t\delta}{\tau}$, where D_e is the effective diffusivity, D the regular one (both in $m^2 s^{-1}$, and ϵ_t , δ , τ are respectively the porosity, the constrictivity and the tortuosity of the porous medium (Grathwohl, 1998), and all are dimensionless.

The porosity captures the fact that the more pores there are then the more possible directions there are for one particle to diffuse. The tortuosity describes almost the same phenomenon: the diffusion is faster in a straight direction than in a tortuous one. Finally, constrictivity models the loss of speed due to the narrowing of the effective size of the pores.

3.7.3 Fluid dynamic equations for the gas phase

In composting it is common feature to force airflow with a fan. The release of heat from the biomass, however, also creates free convection due to buoyancy of the heated air. The airflow induced by free convection can be even greater than that due to the fan. In some cases, there is no forced convection and the renewal of oxygen is provided solely by free convection (Yu et al., 2005).

Main equations. In order to model the fluid dynamics, the Navier-Stokes equations were used with the addition of the Brinkman equations, which model the

complexity of the porous medium (Eq. 3.9) (COMSOL AB, 2008).

$$\frac{\rho}{\epsilon} \frac{\partial \vec{u}}{\partial t} + \frac{\eta}{\kappa} \vec{u} = \vec{\nabla} \cdot \left[-p \mathbf{I} + \frac{1}{\epsilon} \left\{ \eta \left(\vec{\nabla} \cdot \vec{u} + \left(\vec{\nabla} \cdot \vec{u} \right)^T \right) - \frac{2}{3} \eta \left(\vec{\nabla} \cdot \vec{u} \right) \mathbf{I} \right\} \right] + \vec{F} \quad (3.9)$$

... where η denotes the dynamic viscosity of the fluid ($kg\ m^{-1}\ s^{-1}$), \vec{u} is the velocity vector ($m\ s^{-1}$), ρ is the density of the fluid ($kg\ m^{-3}$), p is the pressure (Pa), ϵ is the porosity (unitless), and κ is the permeability of the porous medium (m^2). The influence of gravity and other forces can be accounted for via the force term per unit of mass \vec{F} ($kg\ m^{-2}\ s^{-2}$). \mathbf{I} is the identity matrix of size 2×2 , as the model is implemented in two dimensions. The symbol $\left(\vec{\nabla} \cdot \vec{u} \right)^T$ means the transpose of $\vec{\nabla} \cdot \vec{u}$. In this model the only external force accounted for was the gravitation, because it is the force behind free convection. The term for \mathbf{F} , therefore, is:

$$\mathbf{F} = \begin{cases} F_x = 0 \\ F_y = -g(\rho - \rho_0) \end{cases} \quad (3.10)$$

... where g is the acceleration due to gravity ($m\ s^{-2}$), ρ is the density of the air at a specific location, as in Eq. 3.9, and ρ_0 is the inlet air density (both in $kg\ m^{-3}$).

Density of air. The dependency of ρ on temperature and pressure and that of η on temperature were implemented using the COMSOLTM library.

$$\rho = \frac{M_{air} P}{RT} \quad (3.11)$$

... where M_{air} is the molar mass of air ($kg\ mol^{-1}$), R is the ideal gas constant ($J\ K^{-1}\ mol^{-1}$). T and p are respectively the temperature (K) and pressure (Pa) of the air.

Dynamic viscosity of air. The dependency of η with T was implemented on COMSOLTM with a fitted polynomial. More information can be seen in the COMSOL AB (2008) documentation.

Initial conditions. Uniform vertical airflow was presumed to have been established at the beginning of the simulation. Its value can be found in Table 2, as selected from the literature.

Boundary conditions. In order to implement airflow at the inlet of the vessel, a difference in pressure was chosen as a boundary condition at the bottom layer. Implementation of a fixed value for the airflow at the inlet is actually irrational as, with time, the free convection due to the heat will generate more airflow, which may overwhelm any fixed value imposed at the inlet.

In order to find the appropriate pressure difference to generate the base airflow chosen from the literature, the Darcy-Weisbach equation was used:

$$\Delta p = f \frac{L \rho_{air} V^2}{2D} \quad (3.12)$$

...where f is the coefficient of turbulent flow (unitless) and can be computed from the formula $64/Re$, where Re is the Reynolds number of the system. L is the length of the vessel (m), D its diameter (m), ρ_{air} is the density of air ($kg\ m^{-3}$), and V is the expected airflow ($m\ s^{-1}$).

This formula was used to get an approximation of the appropriate value of Δp . As the air was flowing in a porous medium, however, the relation was not perfect. After several tries with different values of Δp , one was chosen that met the requirement (Table 2). The top boundary was assumed to be open, and the sides as walls, impermeable.

3.7.4 Enthalpy of air

Equation 3.9 modelled the movement of air and provided, once solved, the velocity of the air at any point in the vessel. The velocity vectors were then used to model convection for other particles into the gas phase. The fluid dynamics of this system are linked to its temperature, as airflow is produced by the differences in temperature, and thus density, of the air at different positions. Coupled with the fluid dynamic equation is the heat equation of the air (Eq. 3.13). It takes into account the transfer of heat through conduction and convection, as well as the heat transfer between the two phases:

Main equation.

$$\rho_{air} C_{p_{air}} \frac{\partial \theta}{\partial t} - k_{air} \Delta \theta = Q_{ex} - \rho_{air} C_{p_{air}} \langle \vec{u} | \vec{\nabla} \theta \rangle \quad (3.13)$$

Here, θ represents the temperature of air (K), k_{air} the thermal conductivity ($W m^{-1} K^{-1}$), Q_{ex} the heat exchanged with the liquid phase ($W m^{-3}$), ρ_{air} the density of air ($kg m^{-3}$), and \vec{u} the airflow ($m s^{-1}$). $C_{p_{air}}$ is the specific capacity of air ($J kg^{-1} K^{-1}$). This equation takes into account conduction (the left term), convection (the right term), and heat exchange. There is no heat source in the gas phase (Petric and Selimbasic, 2008).

Heat exchange between phases. The heat exchange at the liquid-gas interface comes from convective transfer and the enthalpy associated with the phase change (Petric and Selimbasic, 2008). In order for liquid water to evaporate it needs an energy equal to the latent heat of vaporization to overcome the bonds between molecules of liquid water. This energy is assumed to be entirely drawn from the liquid phase. By opposition, when vapor condenses it releases the same amount of heat into the liquid phase. The enthalpy associated with temperature change following the phase transition is neglected, under the assumption that the air is almost at dynamic equilibrium with the liquid phase, and there is negligible temperature difference. Hence the formula for the heat transfer in the gas phase depends only on the convective transfer:

$$Q_{ex} = h_{trans}(T - \theta) \quad (3.14)$$

...where h_{trans} is the convective heat transfer coefficient ($W m^{-3} K^{-1}$) and represents the convective heat transfer at the liquid-gas interface. In this approximation, the influence of the heat exchange between the two phases due to evaporation and condensation was neglected in the gas phase.

Initial conditions. The air was set to be at T_{ini} uniformly in the vessel.

Boundary conditions. The inlet air was at a temperature of T_{ini} . Any exchange of heat between the air and the walls was considered to be negligible in comparison to the heat lost through the walls by the solid/liquid phase. The outlet was set as an open boundary with a free convective flux.

3.7.5 Heat equations in the liquid phase

Main equation. In the liquid phase, the biomass releases heat as part of its activity. Also, it was assumed that convection can be neglected in the water film around the compost particles. The main reason is that capillary forces reduce the speed of convection. The spatial dependency of temperature in the liquid phase was still taken into account through conduction, heat exchange with the gas phase, and the convection of the air. The heat equation in the liquid was then:

$$\rho_{liq}C_{compost}\frac{\partial T}{\partial t} - k_{liq}\Delta T = -Q_{ex} + Q_{bio} \quad (3.15)$$

...where T is the temperature of the liquid phase (K), ρ_{liq} is the wet bulk density ($kg\ m^{-3}$), $C_{compost}$ is the heat capacity of the wet bulk ($J\ kg^{-1}\ K^{-1}$), k_{liq} is the thermal conductivity of the liquid phase ($W\ m^{-1}\ K^{-1}$), Q_{ex} is the heat exchange with the gas phase ($W\ m^{-3}$, see Eq. 3.16) and Q_{bio} is the heat released by the biomass ($W\ m^{-3}$). As mentioned, the conduction term was still present through $k_{liq}\Delta T$, but the gradient term responsible for the convection was neglected. Here the transfer term takes into account the energy stored or released by the water as it respectively evaporates or condenses:

$$Q_{ex} = h_{trans}(T - \theta) + L_{vap}W_{ex} \quad (3.16)$$

... where W_{ex} is the amount of water exchanged between the two phases ($mol\ m^{-3}$).

Wet bulk density. The wet bulk density depends on several parameters. In this study it was assumed that density varied with moisture content, since this was a dominant influence. The relation between wet bulk density and moisture content was presumed to be (Glancey and Hoffman, 1994):

$$\rho_{liq} = 379 + 542 MC_{w.b.} [kg\ m^{-3}] \quad (3.17)$$

... where $MC_{w.b.}$ is the moisture content. This expression describes the fact, that as water is lost through evaporation, the bulk density decreases.

Wet bulk heat capacity. The heat capacity of compost has been found to depend on the mineral and the moisture content of compost according to Keener et al. (1993). We assumed in this study, however, that it only depended on moisture content as the mineral content was not taken into account. The relation, still according to Keener et al. (1993), was:

$$C_{compost} = 1.48 + 4.18 MC_{d.b.} \quad (3.18)$$

... where $C_{compost}$ is the heat capacity of compost ($J\ kg^{-1}\ K^{-1}$) and $MC_{d.b.}$ the dry basis moisture content ($kg_{water}\ kg_{substrate}^{-1}$).

Heat created by the biomass. The heat created by the biomass depends on its metabolic activity. Heat is a by-product of the oxidation of the substrate by the microorganisms. As the chemical reactions of oxidation are the same throughout the process of composting, the amount of heat released is directly proportional to the amount of substrate oxidized. The release of heat during specific oxidation reactions

is known, so the stoichiometry of the reactions allows one to find a coefficient of proportionality between the amount of substrate oxidized and the heat released.

The heat released by the biomass can also be modelled as proportional to the oxygen consumption by the biomass within the liquid phase, for the same reasons. The diffusion of the oxygen, however, prevents Q_{bio} from being proportional to $\frac{dO_{2dis}}{dt}$ since the latter term takes into account both the consumption and the diffusion of oxygen. Since the change in mass of the substrate is easier to monitor than consumption of oxygen, it was chosen as the reference for many terms throughout the model.

Hence, $Q_{bio} = \Delta H \frac{dS}{dt}$ where ΔH is the heat of oxidation of the substrate ($J kg^{-1}$).

Initial condition. The compost was assumed to be at ambient temperature, 21°C, at the beginning of the simulation.

Boundary conditions. The compost was assumed to be insulated at the top and bottom boundaries, as it was in contact with nothing but air which was at the equilibrium temperature.

The compost was, however, in contact with the walls of the vessel. The exterior of the vessel was at the ambient temperature of 21°C, so heat flux occurred across the walls. The heat flux was modelled as $U (T_{ambient} - T)$ (Liang et al., 2004). U is the linear heat transfer coefficient of the walls ($J K^{-1} s^{-1} m^{-2}$) (Table 2) estimated from the overall heat transfer coefficient of Liang et al. (2004).

3.7.6 Water equations for gas and liquid phases

Introduction to water diffusion in porous media. In a porous medium, the movement of water through diffusion tends to homogenize the water distribution in the compost. The convective movements, however, can lead to problems at the boundaries. For instance, gravity makes the water accumulate at the bottom and leach out of the compost. In order to avoid these problems and simplify the equations, it was assumed that water only diffused through the media. To model this diffusion, the Buckingham-Darcy equation Eq. 3.19 was used according to Wu (2003).

$$J_w = -K(MC_{vol}) \frac{\partial h(MC_{vol})}{\partial x} \quad (3.19)$$

...where J_w is the flux of water in the porous medium ($m s^{-1}$). $K(MC_{vol})$ is the unsaturated hydraulic conductivity ($m s^{-1}$), $h(MC_{vol})$ is the soil matric potential (m). MC_{vol} is the volumetric water content of the media ($m^3 m^{-3}$). This equation can be changed in order to make the differential of MC_{vol} appear (van Genuchten, 1980).

$$\begin{aligned} J_w &= -K(MC_{vol}) \frac{\partial h(MC_{vol})}{\partial x} \\ &= -K(MC_{vol}) \frac{\partial h(MC_{vol})}{\partial MC_{vol}} \frac{\partial MC_{vol}}{\partial x} \\ &= -D_{H_2O_{liq}}(MC_{vol}) \frac{\partial MC_{vol}}{\partial x} \end{aligned} \quad (3.20)$$

Hydraulic diffusivity. The dependence of hydraulic diffusivity on the water content was developed by van Genuchten (1980):

$$D_{H_2O_{liq}}(MC_{vol}) = \frac{(1-m)K_s}{\alpha m(MC_{vol_s} - MC_{vol_r})} \Theta^{1/2-1/m} \left((1 - \Theta^{1/m})^{-m} + (1 - \Theta^{1/m})^m - 2 \right) \quad (3.21)$$

...where $D_{H_2O_{liq}}(MC_{vol})$ is the hydraulic diffusivity of water ($m^2 s^{-1}$). α , K_s and m are parameters (respectively m^{-1} , $m s^{-1}$, unitless). $\Theta = \frac{MC_{vol} - MC_{vol_r}}{MC_{vol_s} - MC_{vol_r}}$ is the normalized water content or effective saturation ($m^3 m^{-3}$). MC_{vol_r} is the residual water content ($m^3 m^{-3}$), i.e. the minimum amount of water in the medium. MC_{vol_s} is the saturated water content ($m^3 m^{-3}$).

Water content. The water content can be related to the concentration of water in the compost as described by:

$$\begin{aligned} MC_{vol} &= \frac{V_w}{V_T} \\ &= \frac{m_w}{\rho_w V_T} \\ &= \frac{H_2O_{liq} M_{H_2O}}{\rho_w V_T} \end{aligned} \quad (3.22)$$

The first line is the definition of volumetric water content, where V_w is the volume of water contained in the total volume V_T (both in m^3). V_w can be expressed as the ratio of mass m_w with density ρ_w . Finally $H_2O_{liq} = \frac{n_w}{V_T}$, where n_w is the number of moles of water contained in a unit volume V_T . M_{H_2O} is the molar mass of water ($kg mol^{-1}$).

As MC_{vol} and H_2O_{liq} are linearly linked, a simple substitution of variables shows that if MC_{vol} follows the first equation below then H_2O_{liq} follows the second.

$$\frac{\partial MC_{vol}}{\partial t} = \vec{\nabla} \cdot \left(D_{H_2O_{liq}}(MC_{vol}) \vec{\nabla} MC_{vol} \right) \quad (3.23)$$

$$\frac{\partial H_2O_{liq}}{\partial t} = \vec{\nabla} \cdot \left(D_{H_2O_{liq}}(MC_{vol}) \vec{\nabla} H_2O_{liq} \right) \quad (3.24)$$

Here, $D_{H_2O_{liq}}$ (see Eq. 3.21) depends on θ and is not a constant, thus the diffusion coefficient must remain within the differentiation operator (See Eq. 3.26).

Main equations. The dynamics of water were modelled with equation Eq. 3.25 for the gas phase and Eq. 3.26 for the liquid phase.

$$\frac{\partial H_2O_{gas}}{\partial t} - D_{H_2O_{gas}} \Delta h_2O_{gas} = W_{ex} - \left\langle \vec{u} | \vec{\nabla} H_2O_{gas} \right\rangle \quad (3.25)$$

$$\frac{\partial H_2O_{liq}}{\partial t} - \vec{\nabla} \cdot \left(D_{H_2O_{liq}}(MC_{vol}) \vec{\nabla} H_2O_{liq} \right) = -W_{ex} - Y_{S \rightarrow w} \frac{dS}{dt} \quad (3.26)$$

$D_{H_2O_{gas}}$ is the coefficient of diffusion of water in the air (in $m^2 s^{-1}$). $Y_{S \rightarrow w}$ is the yield coefficient of the creation of water due to the consumption of substrate by the biomass ($mol kg^{-1}$). Both diffusion and convection were assumed for the gas phase, whereas only diffusion was implemented for the liquid phase, due to the capillary forces that restrain the movement of water within a porous medium. The effective diffusion coefficient in the liquid phase takes this phenomenon into consideration and is not the same as the value of diffusion of free water (van Genuchten, 1980). W_{ex} is the amount of water exchanged between the two phases ($mol m^{-3}$).

Steady-state equilibrium between the two phases. Dual-phase systems tend toward an equilibrium between the concentrations of a specific species in both phases. For water, this equilibrium is regulated by the saturated vapor pressure of water. The saturated vapor pressure in the air will change until, at the limit, its partial pressure reaches the saturated vapor pressure of water.

The saturated vapor pressure of water in a gas phase depends on temperature θ (K), according to the formula from Perry and Green (2007):

$$psat(\theta) = 10^{22.443 - \frac{2795}{\theta} - 1.6798 \ln(\theta)} \quad (3.27)$$

Exchange rate. The speed with which the partial pressure of vapor approaches the equilibrium depends on a transfer rate coefficient. Thus the exchange term takes the form of:

$$W_{ex} = (H_2O_{gas}R\theta - psat(\theta)) HEAVY(H_2O_{gas}) k_{Law} \quad (3.28)$$

...where W_{ex} is the amount of water exchanged between the two phases ($mol\ m^{-3}\ s^{-1}$). k_{Law} is the mass transfer coefficient at the liquid/gas interface for water ($mol\ s^{-1}\ Pa^{-1}\ m^{-3}$), θ is the temperature of the air (K), and R is the gas constant. $HEAVY(H_2O_{gas})$ is a Heaviside function that has the value 1 when the volumetric water content is higher than the residual water content and 0 otherwise (Fig. 3-3). This function models the fact that, in a porous medium, a part of the water is imprisoned due to surface tension and cannot evaporate.

In reality, the less water there is, the stronger are the tension forces, and the intensity of those forces do not have the discontinuity of the Heavyside function. Furthermore, discontinuities slow the solver considerably. Hence a smoother sigmoid function was used: both as a better approximation of reality and also to speed up the simulations (Fig. 3-3).

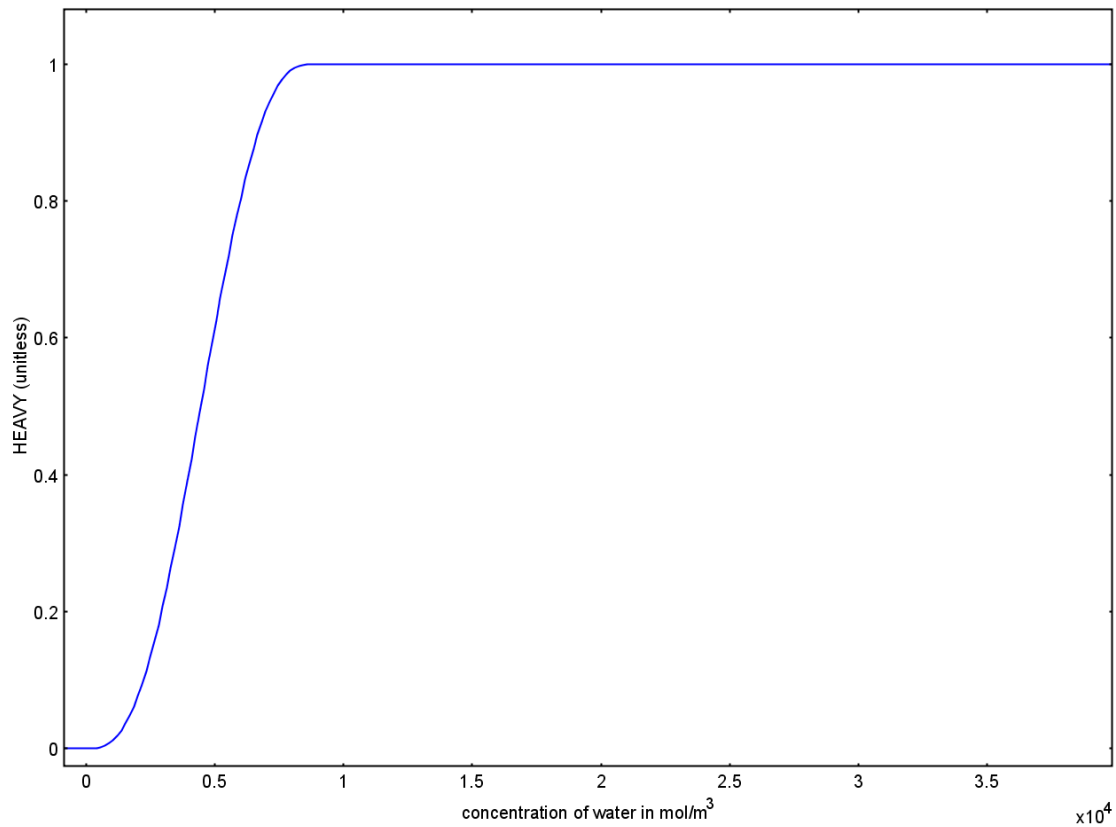


Figure 3-3: Impact of the amount of water on the water exchange between the gas and liquid phase. For this study, the residual water content considered was 400 mol m^{-3} . For low water concentration, surface tension reduces the amount of water exchanged.

Initial conditions. Initially, the water vapour in the air was at the saturated vapour pressure for air at 21°C.

The initial amount of water in the compost was assumed to be that which was mentioned in Stombaugh and Nokes (1996). It was supposed to be uniformly distributed.

Boundary conditions. The water vapour exited freely at the top of the compost due to convective movements of air. At the bottom, the entering air had a partial pressure of water equal to the saturated vapour pressure of water in air at 21°C. The walls were considered to be impermeable to water vapour and liquid mass transfer.

The flux of liquid through all the boundaries was assumed to be null, to model the fact that the water contained in the compost stays within it. Here we assumed that no water leached from the composting matter, which usually is not true in reality.

3.7.7 Oxygen equations for liquid and gas phases

Main equations. The oxygen was consumed by the biomass in the water film. New oxygen was provided by the inlet of fresh air and the convective exchange at the liquid/gas interface. The equations of the dynamics of oxygen in the gas (Eq. 3.29) and liquid (Eq. 3.31) phases were:

$$\frac{\partial O_{2gas}}{\partial t} - D_{O_{2gas}} \Delta O_{2gas} = O_{2ex} - \left\langle \vec{u} | \vec{\nabla} O_{2gas} \right\rangle \quad (3.29)$$

$$\frac{\partial O_{2dis}}{\partial t} - D_{O_{2dis}} \Delta O_{2dis} = -O_{2ex} + O_{2consumption} \quad (3.30)$$

...where D_{O_2gas} and D_{O_2dis} are the respective diffusion coefficients of the oxygen in the gas and liquid phases (both in $m^2 s^{-1}$). D_{O_2dis} is the effective diffusion coefficient in a porous medium.

Oxygen consumption by the biomass. As mentioned, the oxygen consumption is assumed to be proportional to substrate degradation due to consistent stoichiometry.

$$O_{2consumption} = Y_{O_2 \rightarrow S} \frac{dS}{dt} \quad (3.31)$$

...where $Y_{O_2 \rightarrow S}$ is the yield consumption of oxygen ($mol kgS^{-1}$), representing the consumption of oxygen by the biomass. S is the concentration of substrate ($kgS m^{-3}$).

Two films theory. The oxygen exchange at the liquid-gas interface follows Henry's Law: the amount of oxygen in the water is proportional to its partial pressure in the air. In the case of disequilibrium, the difference in local concentrations will initiate the dissolution or evaporation of the molecular species in question.

The mass transfer of a compound between two phases can be modelled according to the two films theory (see Fig. 3-4) (Cussler, 1997). According to that theory, the partial pressure of the compound in the gas phase changes close to the interface. Let us assume that the flow of the compound is from the gas to the liquid phase. In that situation, as the species is transferred at the interface, its partial pressure decreases close to the liquid phase. Some convective transfer happens and some compound is transferred into the liquid phase. It will then diffuse in the liquid, thus decreasing its concentration further away from the boundary. Let p_0 and p_i be the partial pressures (pa) of the compound respectively in the gas phase and at the interface.

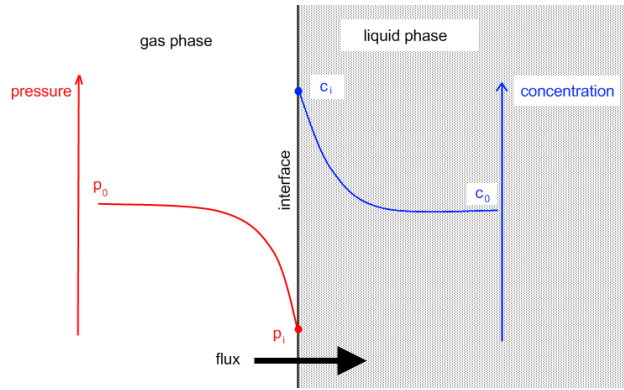


Figure 3–4: Schematic illustrating the two-film theory. The curves are the plots of the partial distributions of partial pressure and concentration of a species in the different phases at the interface. The mass flux is as indicated. Adapted from Cussler (1997)

Let c_0 and c_i be the concentration of the same compound in the gas phase and at the interface (both in mol m^{-3}). The fluxes of the compound from the gas and liquid phase to the interface are, respectively (Cussler, 1997):

$$N_g = k_p(p_0 - p_i) \quad (3.32)$$

$$N_L = k_L(c_i - c_0) \quad (3.33)$$

The flux is in the same direction as the arrow in Fig. 3–4. At equilibrium, there is no accumulation or depletion at the boundary, hence $N_g = N_L = N$ (both in $\text{mol m}^{-2} \text{s}^{-1}$). k_L and k_p are, respectively, the liquid and gas mass transfer coefficient (both in m s^{-1}). p_i and c_i are not easy to measure and to model, however, so in order to use these equations, p_i and c_i need to be removed. Henry’s law states that at the interface between two phases, there is a relation between the partial pressure and

concentration of a compound:

$$p_i = c_i H \quad (3.34)$$

... where H is the Henry's constant for the compound. Using equations Eq. 3.35 and Eq. 3.33, p_i and c_i can be replaced in order to obtain:

$$N = \frac{1}{\frac{1}{k_p} + \frac{H}{k_L}} (p_0 - c_0 H) \quad (3.35)$$

Then we introduce k_{La} , the liquid mass transfer coefficient for oxygen as:

$$\frac{1}{k_{La}} = \frac{1}{k_p} + \frac{H}{k_L} \quad (3.36)$$

... and this formula can be applied to the exchange of oxygen.

Transfer equation.

$$O_{2ex} = k_{LaO_2} (He_{O_2}(T) X_{O_{2dis}} - O_{2gas} R\theta) \quad (3.37)$$

$He_{O_2}(T)$ is Henry's constant ($Pa\ m^3\ mol^{-1}$) for oxygen and depends on the temperature. The mass transfer coefficient ($mol\ s^{-1}\ Pa^{-1}$) of oxygen is k_{LaO_2} (Petric and Selimbasic, 2008).

Molar fraction. The molar concentration ratio of the oxygen in the liquid phase is $X_{O_{2liq}}$ (*unitless*). For a dilute solution, the following equality was assumed:

$$X_{O_{2dis}} = \frac{O_{2dis}}{[H_2O]} \quad (3.38)$$

The molar concentration of pure water, $[H_2O]$, is

$$\frac{\text{mass of water}}{\text{volume of water} * M_{H_2O}} = \frac{1000[g]}{1[L] * 18[g mol^{-1}]} = 55.56[mol L^{-1}] \quad (3.39)$$

Henry's constant. The value of Henry's constant depends on temperature, according to Perry and Green (2007). This dependency was modelled for oxygen with the following equation:

$$He_{O_2}(T) = 101325 \exp\left(66.7354 - \left(\frac{8747.55}{T}\right) - 24.4526 \ln\left(\frac{T}{100}\right)\right) [Pa] \quad (3.40)$$

T is the temperature of the compost (K).

Initial conditions. The air was assumed to contain 21% oxygen at standard pressure (101,325 Pa). The dissolved oxygen in the liquid was at equilibrium with the oxygen in the gas phase according to Henry's law:

$$X_{O_2dis} = \frac{O_{2gas}R\theta}{He_{O_2}(T)} \quad (3.41)$$

Boundary conditions. The concentration of oxygen in the air entering the vessel was also 21%, at standard pressure and a temperature of 21°C. At the top of the vessel, the boundary condition was a convective flux that represented the fact that the vessel was open. The walls were impermeable to air.

As for the oxygen dissolved in the water film, there was no movement of water through any of the boundaries. The water was limited to the water film around the compost particles, so the flux of dissolved oxygen was null at all the boundaries.

3.8 Other processes

The emission of gases (carbon dioxide, ammonia) by the biomass is linearly linked to its activity (e.g. growth) and was not included in this model.

In order to solve this set of partial differential equations, the software COMSOL MultiphysicsTM was used. This software is a commercial solver of 3D problems that are defined with partial or ordinary differential equations.

3.9 Sensitivity analysis

3.9.1 Definition and goals

Definition. The purpose of sensitivity analysis is to determine which input parameters, when varied slightly, most perturb the output of the system. Here, we are studying a function $y = f(i_1, \dots, i_n)$, where y is the output and the i_k are the inputs. The inputs are all the information – e.g. the values of physical constants and parameters – that is required to compute the values of the observed variables of the system. In compost modelling, for instance, the output variables of interest may be the total consumption of oxygen or the time of the peak temperature.

In this study, there was no explicit function f . Instead, f can be considered as the representation of the entire system and the way in which it changes with time. The numerical solution of the mathematical system f is therefore the computation of the estimated values of the output variables of interest over the time history of the system.

Sensitivity analysis aims to find, knowing a starting point in the n -dimensional space of inputs, new point, close to the starting one, that causes the greatest variation in outputs. Since greater perturbations often result in greater deviations, sensitivity

analysis should be limited to a sphere of perturbations where the vector of perturbations is (di_1, \dots, di_n) . This eliminates the effect of change in magnitude, and instead reveal the relative effects of different combinations of inputs. di_k is the perturbation of the k-th coordinate of the new point: its new coordinate is now $i_k + di_k$. The problem lies in finding the vector (di_1, \dots, di_n) that maximizes $dy = f(i_1 + di_1, \dots, i_n + di_n)$ with the condition $\sum_{k=1}^n di_k^2 \leq e^2$, where e is a predefined combined magnitude of the perturbation.

Goals. The functions f that were used for sensitivity analysis were differentiable, but only discrete points were calculated because of required computational resources. The aim of this study was to approximate the most sensitive direction of perturbation (in a n-dimensional input space) with the fewest possible simulations.

3.9.2 Method

First order approximation. Since the system of equations is solved through the resolution of differential equations, the output functions are differentiable, which allows the use of a derivative-based approach for the sensitivity analysis. For such a system, the gradient of the output function serves as the first-order approximation of the direction of maximum change in the output, referenced to the initial point in the space of possible inputs:

$$\vec{grad}(f) = \left(\frac{\partial f}{\partial i_1}(i_1, \dots, i_n), \dots, \frac{\partial f}{\partial i_n}(i_1, \dots, i_n) \right) \quad (3.42)$$

When the function is not analytical, as in this study, the gradient is computed with numerical methods based on the formula:

$$\frac{\partial f}{\partial i_1}(i_1, \dots, i_n) = \lim_{di_1 \rightarrow 0} \frac{f(i_1 + di_1, i_2, \dots, i_n) - f(i_1, \dots, i_n)}{di_1} \quad (3.43)$$

In order to evaluate the limit, one should choose a small enough value for di_1 so that a smaller one would not change substantially change the approximation of the partial derivative. To compute the gradient of the output, at least $n + 1$ simulations are required. This method allows the location of the approximate direction of the most sensitive perturbation in a system of n inputs.

As mentioned, this kind of analysis is restricted to a sphere of perturbations of a chosen radius ϵ . Different input parameters, however, are not necessarily perturbed to the same magnitude. In order to respect the scale of variation for each parameter, a new formalism needs to be adopted: $dy = f(i_1 + \alpha_1 di_1, \dots, i_n + \alpha_n di_n)$ where α_k stands for the maximum perturbation of each parameter and i_k is the scaled perturbation ranging from -1 to 1. The gradient becomes

$$\vec{grad}(f) = \left(\alpha_1 \frac{\partial f}{\partial i_1}(i_1, \dots, i_n), \dots, \alpha_n \frac{\partial f}{\partial i_n}(i_1, \dots, i_n) \right) \quad (3.44)$$

This gradient indicates the approximate direction of the most significant increase on the sphere of scaled perturbations, $\sum_{k=1}^n di_k^2 \leq 1$. The most sensitive perturbation is indicated by the point identified:

$$\frac{1}{\|\vec{grad}(f)\|} \left(\alpha_1 \frac{\partial f}{\partial i_1}(i_1, \dots, i_n), \dots, \alpha_n \frac{\partial f}{\partial i_n}(i_1, \dots, i_n) \right) \quad (3.45)$$

Second order approximation. The gradient indicates the tendency of a perturbation on each input to disturb the output of the system. In this method, however, it is assumed that the effects of two perturbations combine linearly. The first order approximation does not take into account the complexity of a non-linear interactions which might be theoretically modelled by a second-order: $\frac{\partial^2 f}{\partial i_1 \partial i_2}(i_1, \dots, i_n)$.

If a second order term is included, the approximation of the response in the output (dy) with regard to a perturbation in the inputs (i_k) is:

$$dy \approx \underbrace{\sum_{k=1}^n \alpha_k \frac{\partial f}{\partial i_k}(i_1, \dots, i_n) di_k}_{\text{first order}} + \underbrace{\sum_{p=1}^n \sum_{q=1}^n \alpha_p \alpha_q \frac{\partial^2 f}{\partial i_p \partial i_q}(i_1, \dots, i_n) di_p di_q}_{\text{second order}} \quad (3.46)$$

The maximum of that perturbation on the unit sphere of (di_1, \dots, di_n) can be found using Lagrange multiplication or any method that finds the minimum of a function under an equality constraint.

Eq. 3.43 gives a discrete approximation of the first-order derivatives. The following equations can be used to compute second-order partial derivatives using the same technique:

$$\frac{\partial^2 f}{\partial^2 i_1}(i_1, \dots, i_n) = \lim_{di_1 \rightarrow 0} \frac{f(i_1 + 2di_1, i_2, \dots, i_n) - 2 * f(i_1 + di_1, i_2, \dots, i_n) + f(i_1, \dots, i_n)}{di_1^2} \quad (3.47)$$

$$\lim_{(di_1, di_2) \rightarrow (0,0)} \frac{\frac{\partial^2 f}{\partial i_1 \partial i_2}(i_1, \dots, i_n) = \frac{f(i_1+di_1, i_2+di_2, i_3, \dots, i_n) - f(i_1+di_1, i_2, \dots, i_n) - f(i_1, i_2+di_2, i_3, \dots, i_n) + f(i_1, \dots, i_n)}{di_1 di_2}}{(3.48)}$$

3.10 Assumptions

- The vessel was assumed to be a channel with a rectangular cross-section, and so a two-dimensional rectangle was used as a model of the three-dimensional vessel.
- The edge effects due to the extremities of the vessel were considered to be negligible.
- The supply of air from the bottom of the vessel was uniform across the bottom of the compost bed.
- The vessel was taller than the compost it contained. There was always a column of free air above the compost before the air was exhausted. This assumption prevented any boundary conditions at the top border of the compost other than convective flux.
- Biological activity was entirely aerobic.

- Diffusion in the porous medium could be modelled with Fick's Second Law given an appropriate diffusion coefficient.
- The solid and liquid phases of the compost substrate were modelled as a single phase, for the sake of simplicity. The parameter values were usually taken as the mean of those for the solid phase and the water film.

CHAPTER 4

Results

COMSOL MultiphysicsTM was used to solve the stated modelling problem with regard to time and space. Using this implementation of the model, it was possible to follow the evolution of each parameter over time at any point in the composting vessel, and even to generate a color map of a slice of the vessel for any parameter.

This study was not meant to be validated against any physical experiment, but rather as a basis for further applied models. This model did not describe any existing compost data but described the general behavior of compost. The main reason for this is that no published data included the values for all the constants and parameters needed for the model in this study.

4.1 General behavior

4.1.1 Temperature

Pattern over time. The evolution of the temperature of the liquid and the gas phases was similar (see Fig. 4-1 and 4-2). This similarity was because of the fast heat exchange rate between the two phases and the slow airflow, which allowed enough time for the heat exchange to establish steady state between the phases. The bulk temperature was considered in this analysis. The evolution of the temperature followed a similar trend everywhere in the compost, though differences were observed in several aspects (see Fig. 4-1).

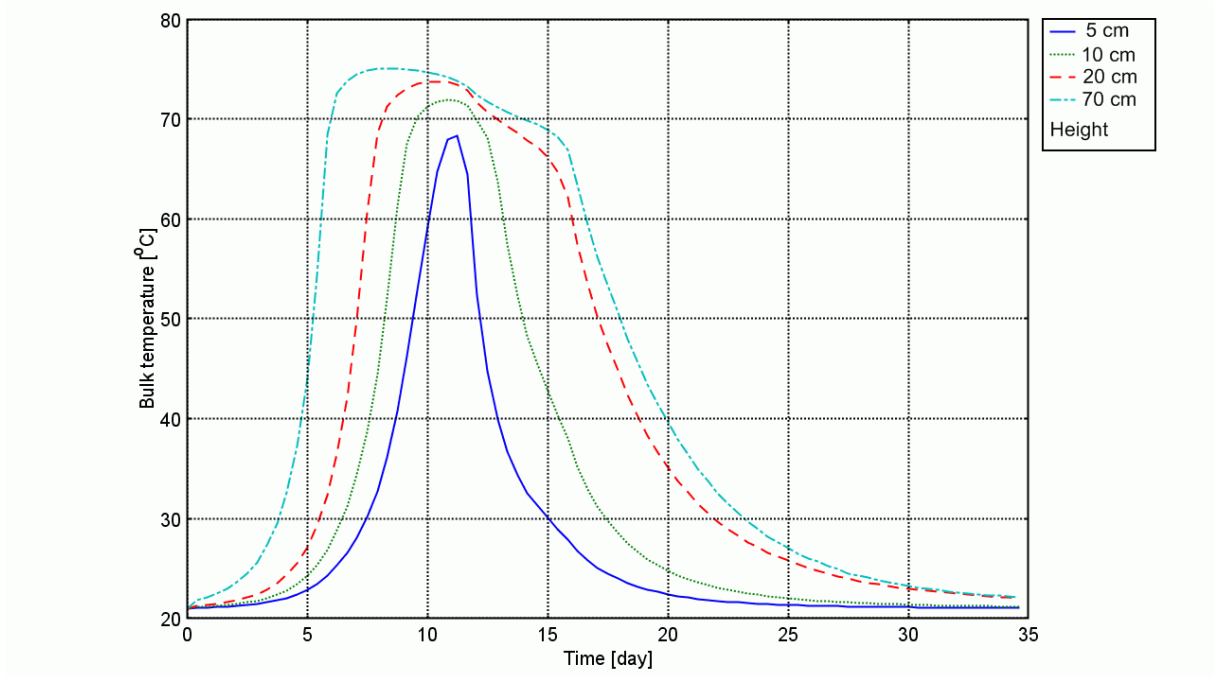


Figure 4-1: Pattern of variation of bulk temperature with time at several heights in the center of the rectangle representing the composting bed.

The general pattern observed was a rise in temperature after an initial delay. The rise was exponential and stopped when the temperature reached about 75°C. The delay was between 2 and 3 days but depended on the position in the compost: the rise happened faster at the top of the barrel than at the bottom. Following this rise was a period where the temperature plateaued. The length of this plateau was longer at higher positions. Afterward, the temperature decreased exponentially until it reached that of the ambient inlet air. The decrease was slower close to the top of the compost. At the bottom of the compost, because of the inlet of fresh, cool air,

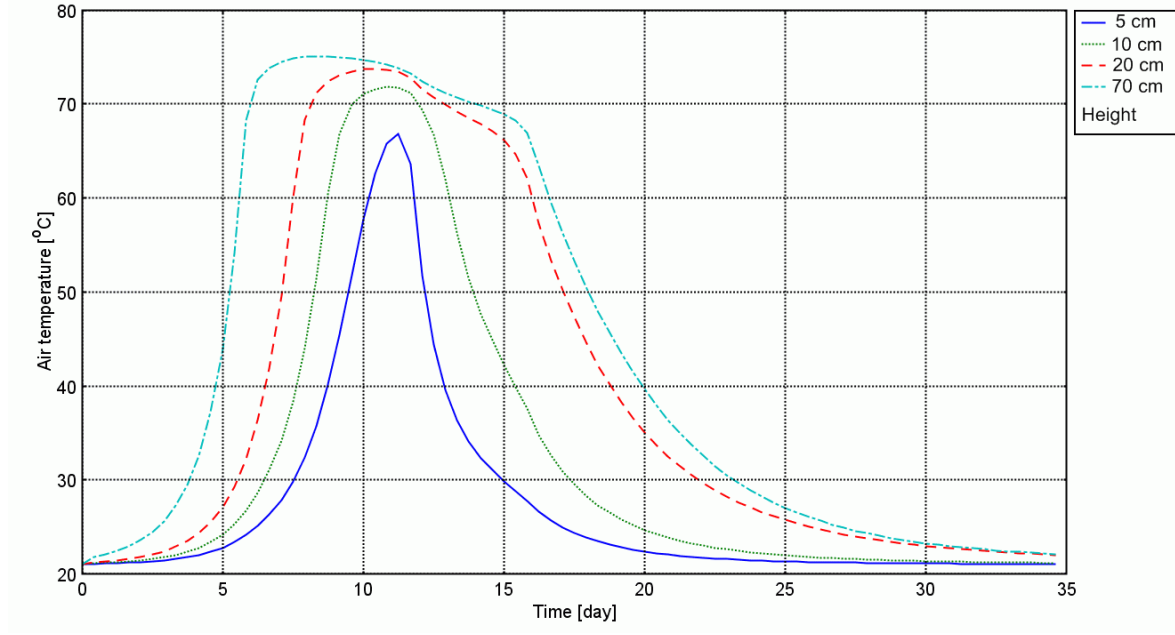


Figure 4-2: Pattern of variation of gas temperature with time at several heights in the center of the composting bed.

the temperature was low and inhibited any biomass activity, therefore the substrate was not consumed at the bottom of the compost.

This phenomenon, typical of compost, is explained by the growth of the biomass. The growth of the biomass releases heat which further enhances the growth of biomass until high temperatures inactivate the enzymes of the biomass. The biomass then maintains the temperature at those high values until the substrate, water, or oxygen is depleted. In this study, the main limiting factor was the water content. When that limited resource is depleted, the biomass activity is reduced and the temperature decreases to the inlet temperature.

Spatial dependency. The temperature initially increased faster at the top of the vessel. Once the top of the vessel reached the plateau, the maximum temperature front moved down until almost all of the compost was at that temperature (see Fig. 4–3). Only the bottom remained cool because of the influence of the inlet of air at 21°C. Because of this low temperature, very few changes occurred at the bottom.

The front stayed close to the bottom for a bit more than one day, then moved up by a small amount: less than 10 cm. When the front stopped moving, the temperature decreased almost uniformly throughout the compost above the front, even though the front itself remained as a high temperature gradient.

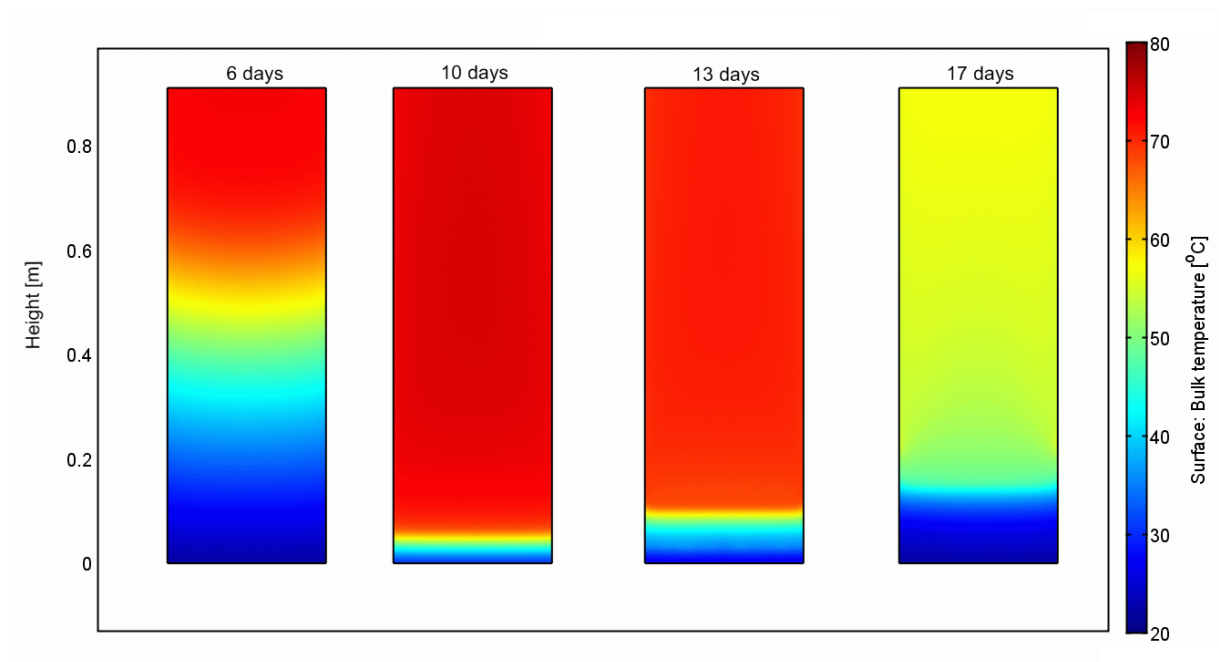


Figure 4–3: Pattern of variation of bulk temperature in a vertical slice of the compost bed.

The lowest position of the front was determined by the temperature and velocity of the inlet air. The closer to the inlet, the supply of oxygen was greater, which enhanced biomass activity, but the air was also cooler closer to the inlet. The front occurred where the combined influence of these two functions was maximized. The biomass activity developed in this zone until the substrate was depleted. As the substrate was depleted, the location of maximum biological activity moved upward. If the inlet temperature was constant, the consumption of oxygen decreased almost to zero below the front where there was no more biomass, while the upper positions still had enough oxygen for biomass to grow.

This front phenomenon stopped when the water was depleted in the vessel, at which point the biomass activity was inhibited by the lack of water. After this time, the biomass could not generate enough heat to maintain an elevated temperature, and the compost cooled to ambient temperature.

This pattern allowed the definition of the three zones. The lower zone included the compost situated from the bottom of the vessel to the lowest position of the front. The middle zone extended from the lower position of the front to its final position. The upper zone was above the uppermost position of the front.

4.1.2 Biomass

Pattern over time. Several patterns of behavior were observed in the concentration of the biomass (see Fig. 4-4).

At a height of 20 *cm*, after a small delay, the biomass concentration increased to a maximum value after 7 days and then decreased. Around day 17, there was another increase in biomass, but then it quickly fell to almost zero. The increase

happened when the temperature front stopped moving and before the temperature began to decrease. The behavior was the same higher in the compost.

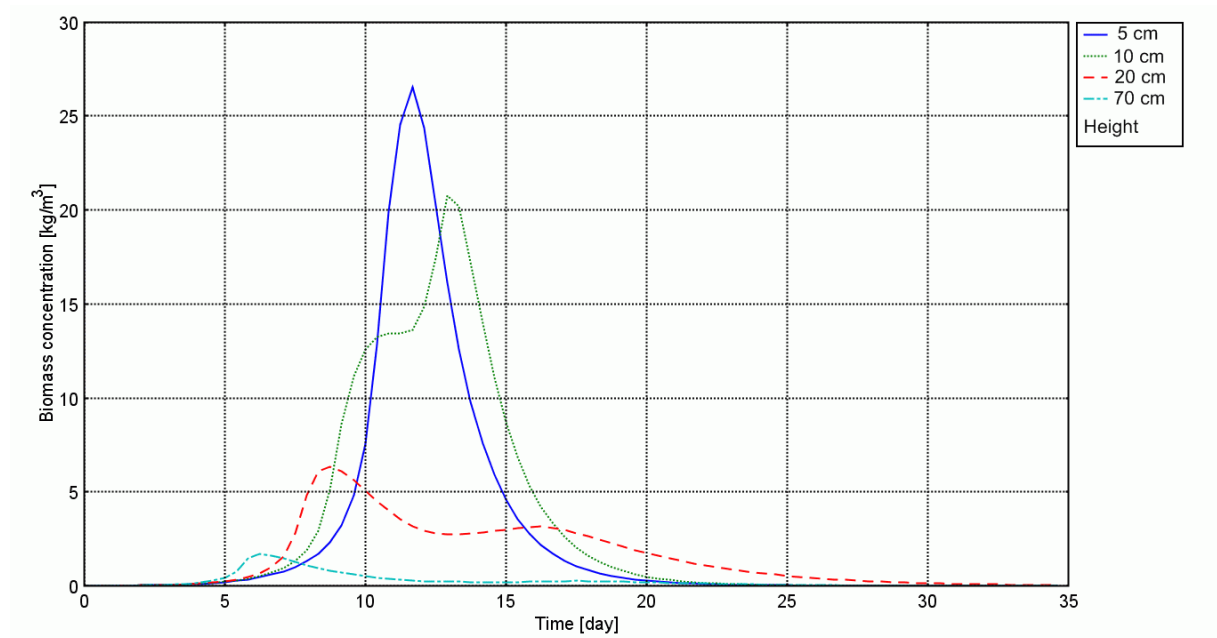


Figure 4–4: Pattern of variation of biomass concentration with time at several heights in the center of the composting bed.

In the middle zone of the compost, the biomass first grew but then stopped for a short time until new growth occurred. The first growth of the biomass occurred before the temperature became too high, i.e. before the temperature front passed the given location. The second growth happened when the temperature front returned upward because of the lack of substrate at lower positions.

In the lower zone of the compost, the biomass concentration increased up to a maximum that was lower than in the other zones, then decreased.

Spatial dependency. At first, the largest increase in the biomass was at the top of the vessel (see Fig. 4–5). When the maximum temperature was reached, the biomass started to decrease at the top of the vessel while it was still increasing at lower positions. As a result, a belt of more concentrated biomass appeared. This belt moved downward, following the location of the maximum temperature.

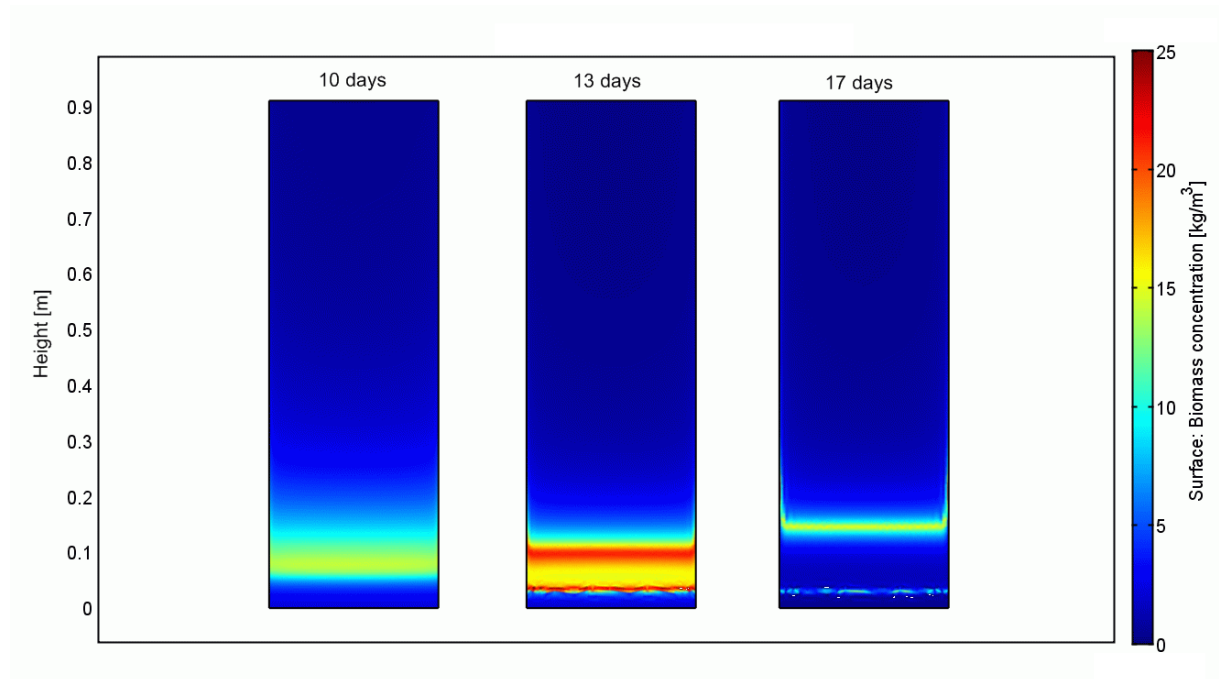


Figure 4–5: Pattern of variation of biomass concentration with respect to height, in a vertical slice of the compost bed. Day 6 is not shown because the biomass concentration on day 6 was very small in comparison to days 10, 13 and 17.

The belt of high biomass concentration stabilized just above the bottom of the vessel when the temperature front did so. When the substrate was depleted at that depth, the belt followed the temperature front upward and stopped when water became a limiting factor.

4.1.3 Substrate

Pattern over time. The same pattern in substrate concentration happened everywhere in the compost bed: at first it remained constant, then decreased exponentially to a stable value (see Fig. 4-6). This final value depended to a great extent on the depth, as the substrate loss varied between 5% to almost 100%.

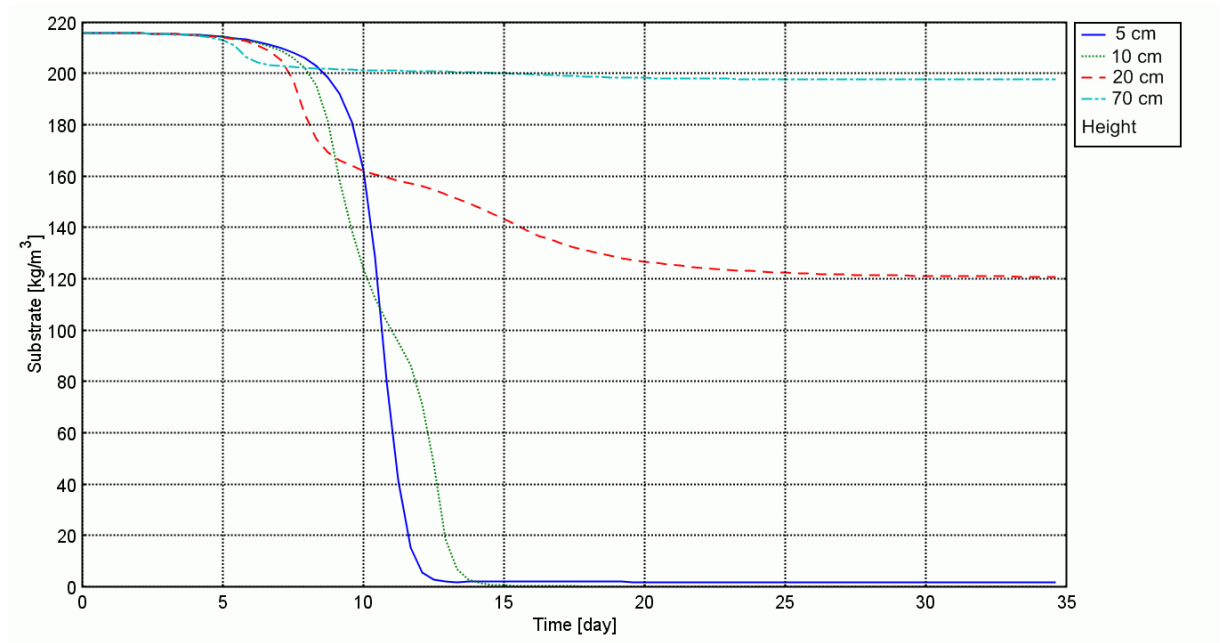


Figure 4-6: Pattern of variation of substrate density with time at several heights in the center of the compost bed.

Spatial dependency. The substrate concentration was negatively correlated with the biomass activity, so the substrate was depleted at first at the top of the vessel (Fig. 4-7). As the temperature reached 75°C at the top, the substrate was preferentially consumed at greater depth. It took longer for the temperature to reach its maximum at greater depths, resulting in a downward-moving belt of reduced

substrate concentration. When that belt reached its lowest position, the substrate was totally depleted. As the biomass activity then moved upward again, the zone of total depletion of the substrate likewise moved upward.

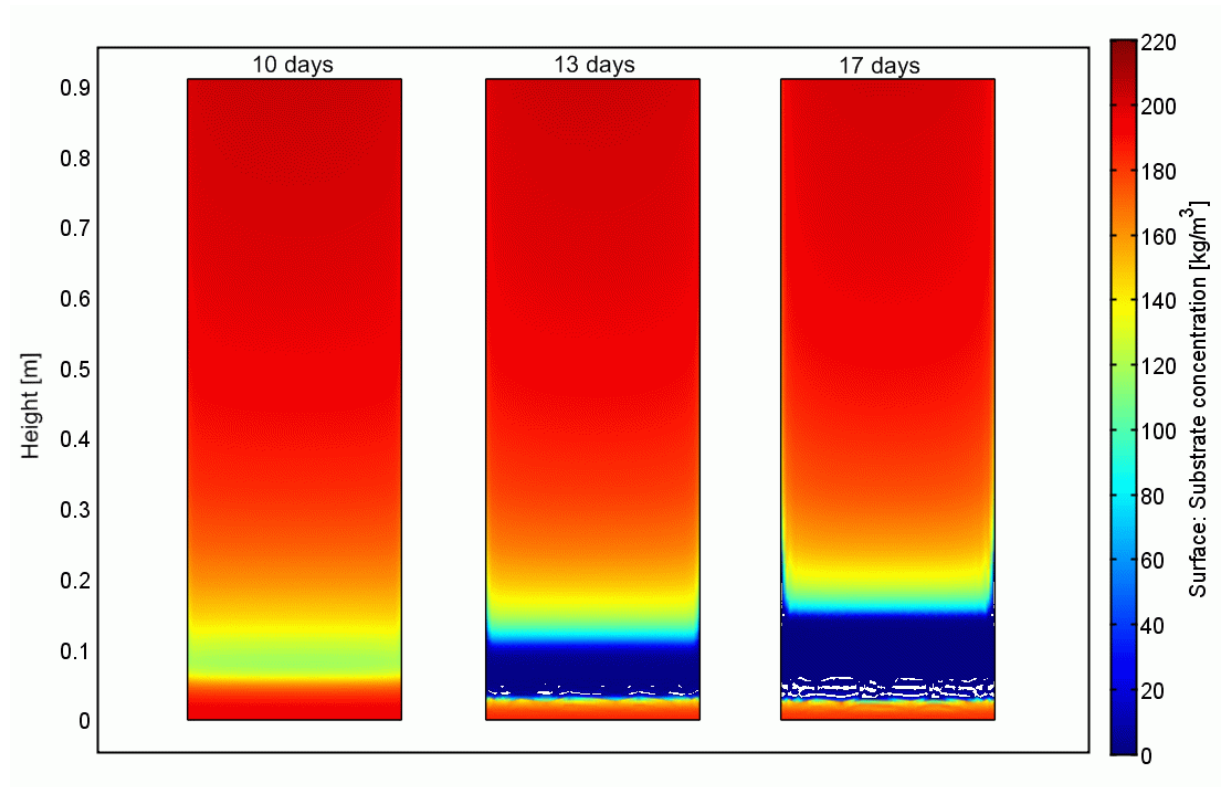


Figure 4-7: Pattern of variation of substrate density in a vertical slice of the composting bed. The gradient in the substrate density was extremely large, ranging from 200 kg m^{-3} to zero in few centimeters, so the mesh size of the finite element mode was not small enough to smoothly capture the variation of the substrate. Hence, the small white band represents mesh elements where the gradient was so strong that the solver gave a negative solution. A smaller mesh size would have solved this problem, but such a change would also have greatly increased the time required for the simulations.

4.1.4 Oxygen

Pattern over time. The changes in the oxygen concentration in the liquid and gas phases of the compost were strongly correlated, because the low air velocity allowed near steady-state between the concentrations in those two phases (Fig. 4–8 and 4–9). As the oxygen consumption depends on the biomass activity, the general pattern of oxygen concentration was an initial delay, a large decrease, and a return to the original concentration when the biomass activity ceased.

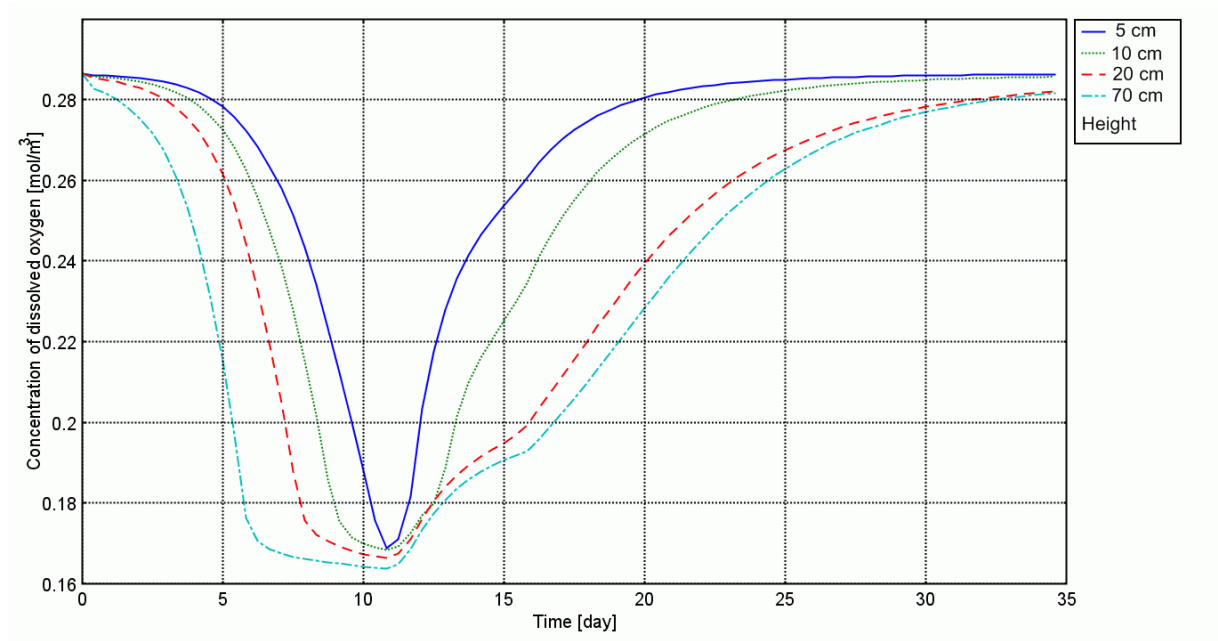


Figure 4–8: Pattern of variation of dissolved oxygen in water with respect to time at several depths in the center of the compost bed.

The airflow in the gas phase was upward, so that any depletion of oxygen at greater depth also caused a subsequent decrease at lesser depth. Thus the return to the original concentration at these lesser depths was not as fast as the initial decrease.

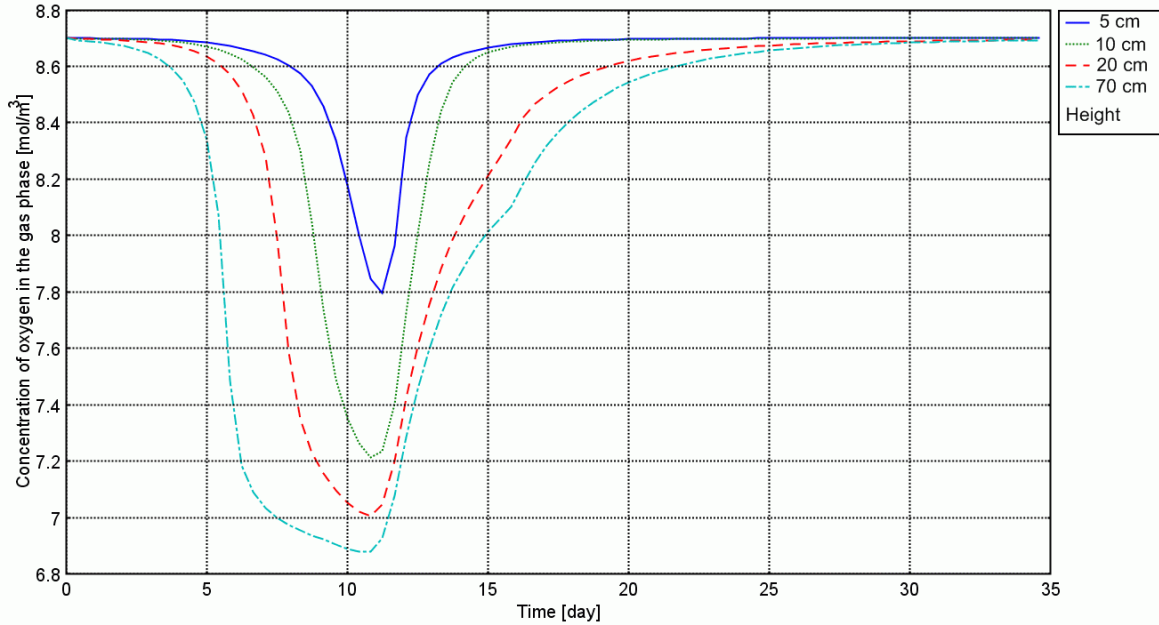


Figure 4-9: Pattern of variation of oxygen in the gas phase with respect to time at several depths in the center of the compost bed.

This pattern was especially pronounced in the liquid phase which, in addition to this problem, was supplied only through mass transfer between the two phases, thus slowing even further the recovery of oxygen.

Spatial dependency. Since oxygen was supplied by fresh air from the bottom of the vessel, the spatial dependency of changes in oxygen concentration was well described by a two-case scenario. At positions below the belt of concentrated biomass, the oxygen concentration was high. In contrast, above this belt, the concentration of oxygen was low. An strong gradient could be seen in the belt where the biomass was concentrated (Fig. 4-10).

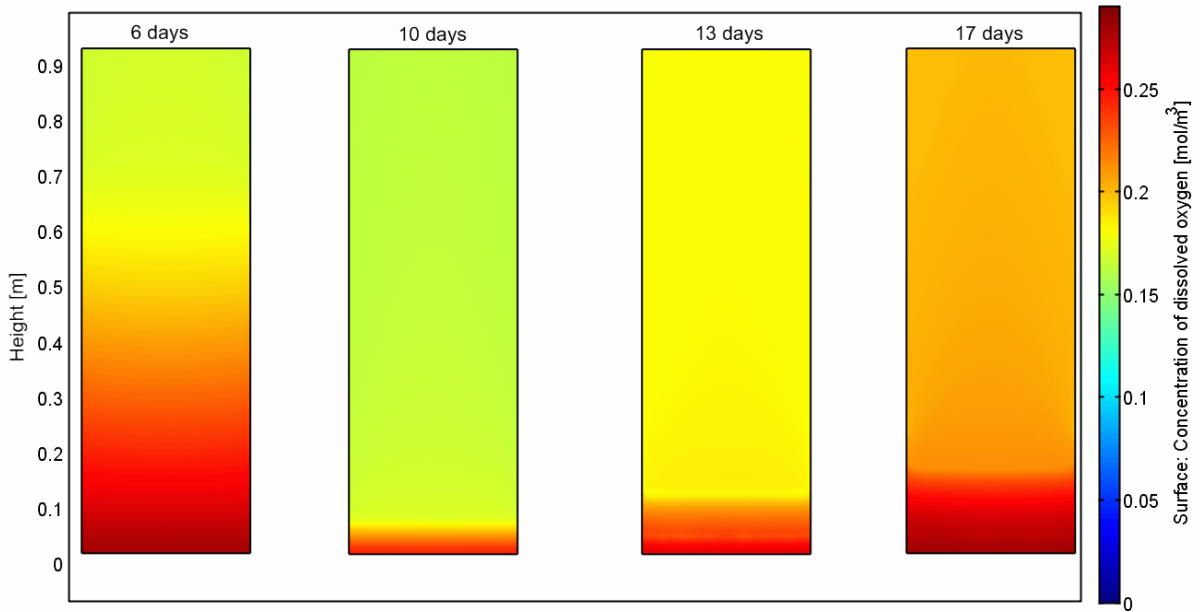


Figure 4–10: Pattern of variation of dissolved oxygen in water with respect to height in a vertical slice of the compost bed.

The movement of the belt of concentrated biomass was followed by a corresponding repartition of the oxygen concentration. See the description of the biomass activity for further details.

4.1.5 Water

Pattern over time. Liquid water was similarly depleted over time at all points in the compost (Fig. 4–12). The pattern of depletion was similar to that of the substrate: after an initial period of stagnation, a sigmoidal decrease occurred. The concentration of water did not drop to zero, because matric forces and hydraulic

pressure forced a minimum amount of water to remain in the porous medium even in a dry environment.

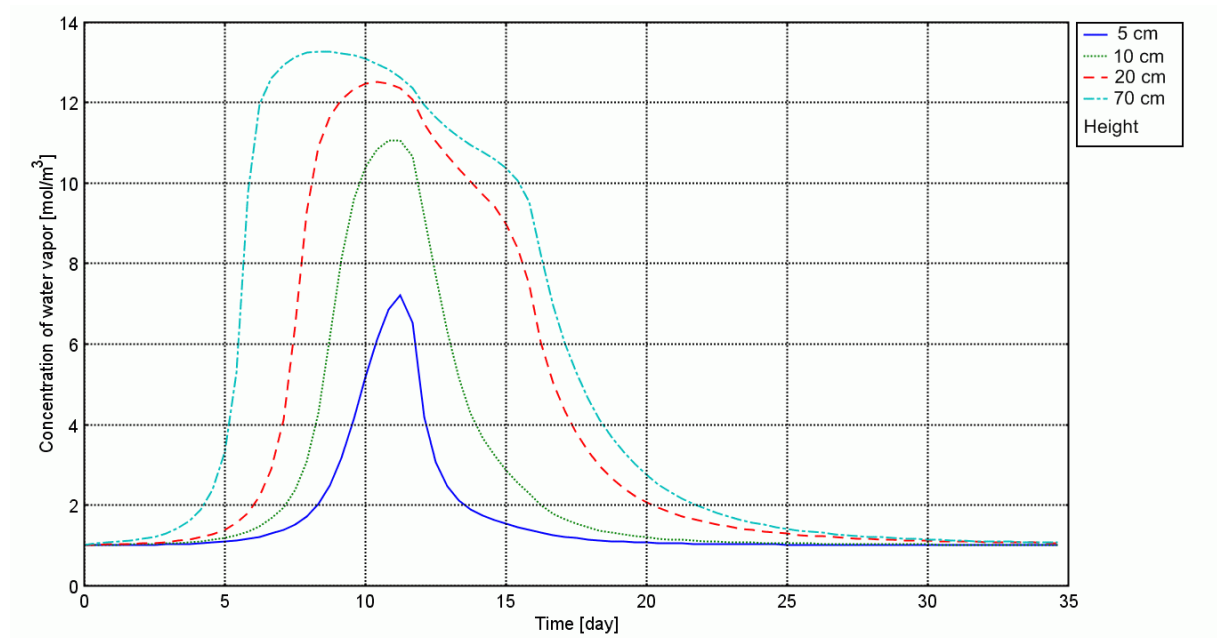


Figure 4–11: Pattern of variation of water vapor with respect to time at several depths in the center of the compost bed.

The water vapor concentration followed the change in temperature, since the low air velocity resulted in a vapor concentration close to the saturated vapor pressure (Fig. 4–11). The partial pressure of water, however, dropped to that of ambient air when a depressed concentration of liquid water no longer allowed evaporation.

Spatial dependency. Liquid water evaporated until a steady state was established, as determined by the saturated vapor pressure in the gas phase. Temperature increased first at the top of the compost, resulting in the greatest drop in liquid water concentration. When the temperature front moved downward, the liquid water

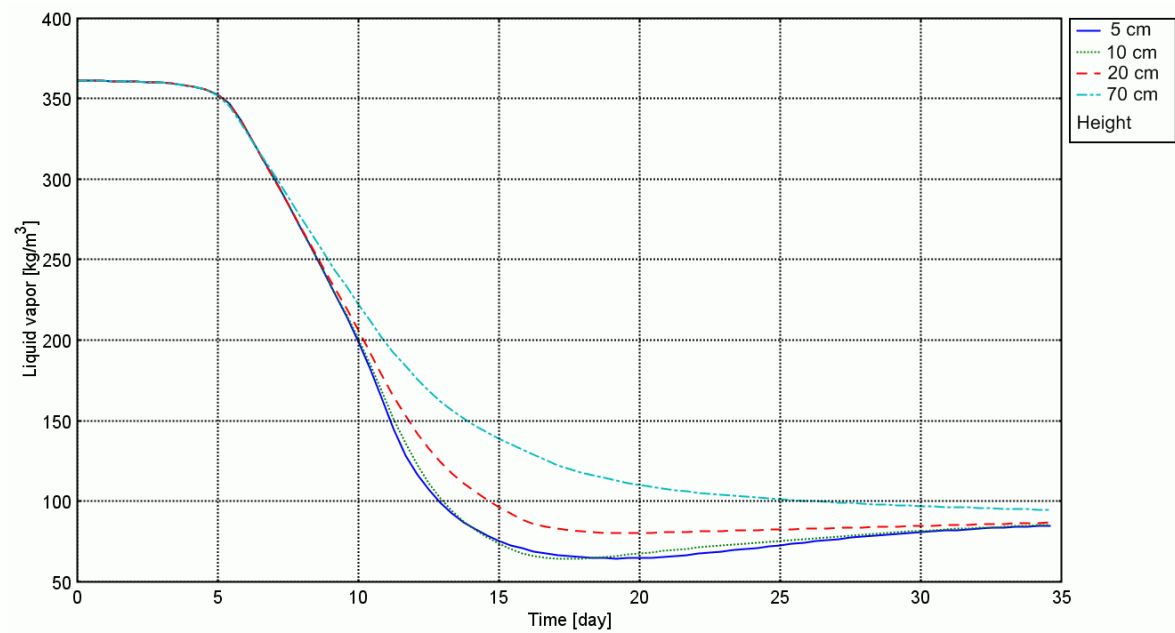


Figure 4-12: Pattern of variation of liquid water with time at several heights in the center of the composting bed.

of the front evaporated to establish steady-state. As the air traveled upward, the partial pressure of water was almost at equilibrium. The decrease in liquid water concentration in the upper region of the compost was then less than that near the temperature front. Hence, the distribution of liquid water rapidly changed from more water at greater depth to more water at less depth. This distribution remained the same until the end of the simulation. No spatial graph is shown for this variable because the decrease was almost uniform in the compost.

4.2 Impact of initial concentration of water

4.2.1 Experimental procedure

In order to test the impact of the initial concentration of water on different parameters, the following initial concentrations were used (in percentage of the initial value): 50%, 60%, 70%, 80%, 90%, 150%, 200%, 300% (Table 2).

4.2.2 Higher initial concentration

The lack of liquid water was the limiting factor that stopped the progression of the temperature front toward the top of the vessel. When water became scarce, the temperature started decreasing above the front to reach ambient. Adding more water delayed its depletion, hence the front moved even further upward before stopping.

Effects on temperature. When the initial concentration of water was higher, the temperature front stopped later, the front moved to a higher position, and the maximum temperature at the top of the compost was maintained longer.

Effects on the biomass. Given more water, the growth of the biomass lasted longer and the belt of concentrated biomass moved higher in the compost, as did the temperature front. Thus, the overall quantity of biomass produced during the process increased.

Effects on the substrate. For the same reasons as stated above, the zone in which the substrate was totally depleted extended even further toward the top of the compost. More substrate was consumed during composting when the initial amount of water was increased.

Effects on oxygen concentration. The position of the highest gradient in oxygen concentration was the same as that of the belt of biomass accumulation, so its position kept moving upward so long as some water was still available.

Effects on the water. The pattern of change in liquid water concentration was not affected by the initial concentration of water; the only difference was a scaling effect due to the increase in initial concentration.

4.2.3 Low initial moisture content

Lower initial concentrations of water slowed composting.

Effects on Temperature. The water was depleted earlier when initial water concentration was lower, and the combined impact of the moisture content, temperature and oxygen was maximized. Thus, the point where the motion of the temperature front reversed was higher than when the initial water content was greater. The temperature front did not move downward as far as with the initial water content before perturbations.

Effects on biomass. The aforementioned effect caused the zone of complete depletion of the substrate to move upward. Accordingly the belt of concentrated biomass moved less than with a more important initial concentration of water.

Effects on substrate. The effect, as mentioned above, led to a depletion in substrate higher in the compost.

Effects on oxygen. When the initial moisture content was lower, the depletion of oxygen did not last as long as with higher initial concentrations of water. Hence, a lower initial concentration of water resulted in a more rapid return to the ambient concentration of oxygen.

Effects on water. The minimum concentration of water was reached faster when the initial water concentration was smaller than when the initial water concentration was greater.

4.2.4 Effect of initial moisture content on final substrate density

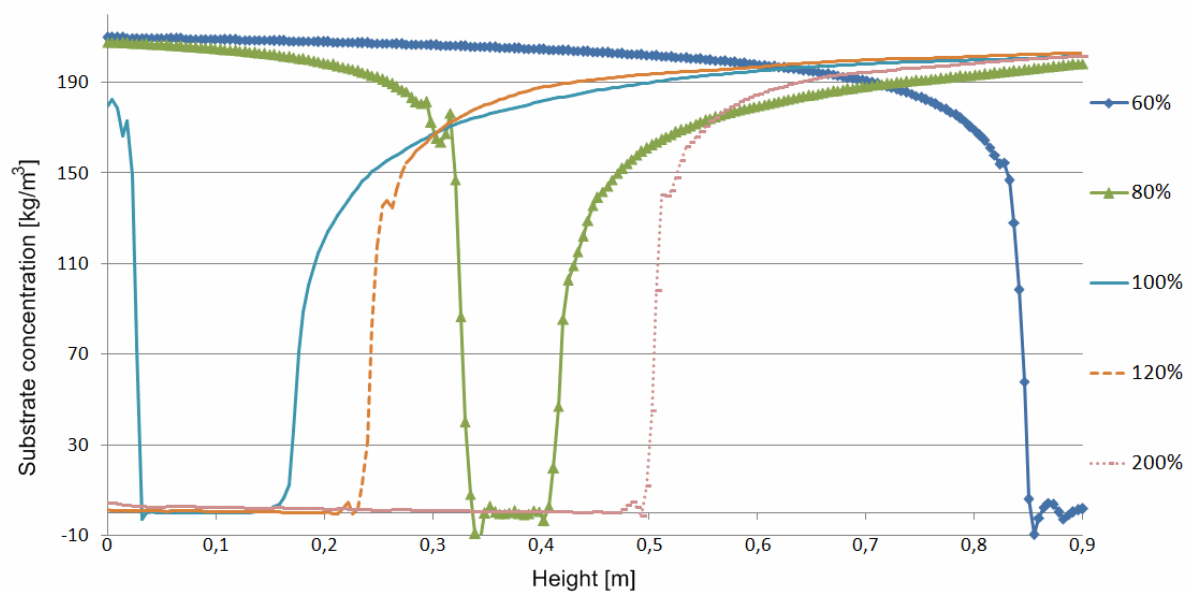


Figure 4–13: Final spatial distribution of bioavailable substrate concentration with regards to different initial concentration of water. The initial concentrations of water are indicated in proportion of the value from Table 2. The concentration of substrate is sometimes negative close to the highest gradient of water concentration. This phenomenon is due to the fact that the mesh size was too great to smoothly capture the variation of the substrate. Reducing the mesh size would solve the problem but increase the simulation time.

Fig. 4–13 shows the impact of the initial water content on the final substrate density. The areas where the substrate was totally depleted had sustained high biomass activity: this was the zone between the two stops of the temperature front. This figure shows that, when there was not enough water, the front did not move

down to the bottom of the compost bed. When there was enough water, however, the front reached the bottom and depleted the substrate from the bottom to the second stop of the temperature front, which was located higher in the compost bed when the initial water concentration was greater.

4.3 Impact of airflow

4.3.1 Experimental procedure

The differential pressure across the inlet fan was $300Pa$. In this study differential pressures of 1, 10, 100, 500, 1000 Pa were investigated. Those differential pressures were very low, the reason being that the airflow is also very low. In actual systems, the airflow is not as low as simulated here, but is instead turned on and off, so that the mean air flow corresponds to the differential pressures used here.

4.3.2 Higher airflow

A greater airflow evacuated the heat from the compost faster. Moreover, it increased evaporation as more fresh, dry air came from the inlet, and more water was required to reach a steady state vapor balance. The flux of water at the interface between the two phases was thus greater when airflow was higher. This implies that the depletion of water from the compost was more pronounced. The supply of oxygen, however, was more efficient, meaning that during the time when there was adequate water the activity of the biomass was boosted. In general, the biomass activity was more important but during a shorter period of time.

Effects on temperature. Three effects of higher inlet air pressure – more water evaporation, a higher airflow and more oxygen supply – played a role in the downward progression of the temperature front. With greater airflow, the location

of the first stop of the temperature front moved upwards. With very large airflow, the depletion of the liquid water was faster than the propagation of the temperature front, which was stopped earlier than for lower airflow.

Effects on biomass. The area of higher concentration of biomass moved downward less when the airflow was stronger, for the reasons mentioned above.

Effects on substrate. For the aforementioned reasons, the area of total depletion of substrate was restricted to lower depths with greater airflow, as compared to lesser airflow.

Effects on oxygen. The change in position of the temperature front, resulted in the consumption of oxygen at greater depths. Once the biomass activity stopped, the higher airflow insured a faster recovery at the top than with lower airflow.

Effects on water. The water was expelled faster with greater airflow than with lower airflow. More water vapor was needed for the steady state and the evaporation of water increased with the airflow. Hence, the overall depletion of water was faster with a greater airflow.

4.3.3 Lower airflow

Effects on temperature. At lower airflow, the air was evacuated at a slower rate and less fresh air entered at the inlet, resulting in a faster increase in temperature. Also, the depletion of liquid water due to evaporation was reduced when less dry air entered the compost. The front of high temperature reached the bottom of the compost bed faster. Once the temperature front reached the bottom of the compost, the change in temperature was slower. This was because the lack of oxygen slowed down the biomass activity.

Effects on biomass. With decreased airflow, movement of the concentrated biomass from the top to the bottom of the compost bed was faster due to increased temperature. Once the biomass was concentrated at the bottom of the compost, the spatial pattern of the biomass stabilized. As the supply of oxygen decreased with the airflow, the biomass activity was inhibited and thus needed a longer time to deplete the substrate at the depth where the biomass was concentrated. The upward motion of the belt of concentrated biomass was also slower because of the same effect.

The slower motion of the concentrated biomass caused a new phenomenon to appear. Usually, above the temperature front, the biomass activity was totally inhibited due to extreme temperature. In the areas close to the walls, however, the heat loss to the exterior actually cooled down the compost enough to enable some biomass growth. The small supply of oxygen made this process slow, which is why it was not obvious in other simulations. It should be noted that the high, yet not extreme, temperatures were critical for this phenomenon to happen. Indeed, a low temperature coupled with a low supply in oxygen would have prevented any biomass growth.

The pattern of biomass concentration was no longer a belt, but took the shape of a U (see Fig. 4-14). As the substrate was depleted at the bottom of the compost bed, the height of the U was reduced and, likewise, as the substrate was depleted close to the walls the width of the U was also reduced.

Effects on substrate. The depletion of the substrate followed the areas of high biomass concentration. For the reasons mentioned in the preceding paragraph,

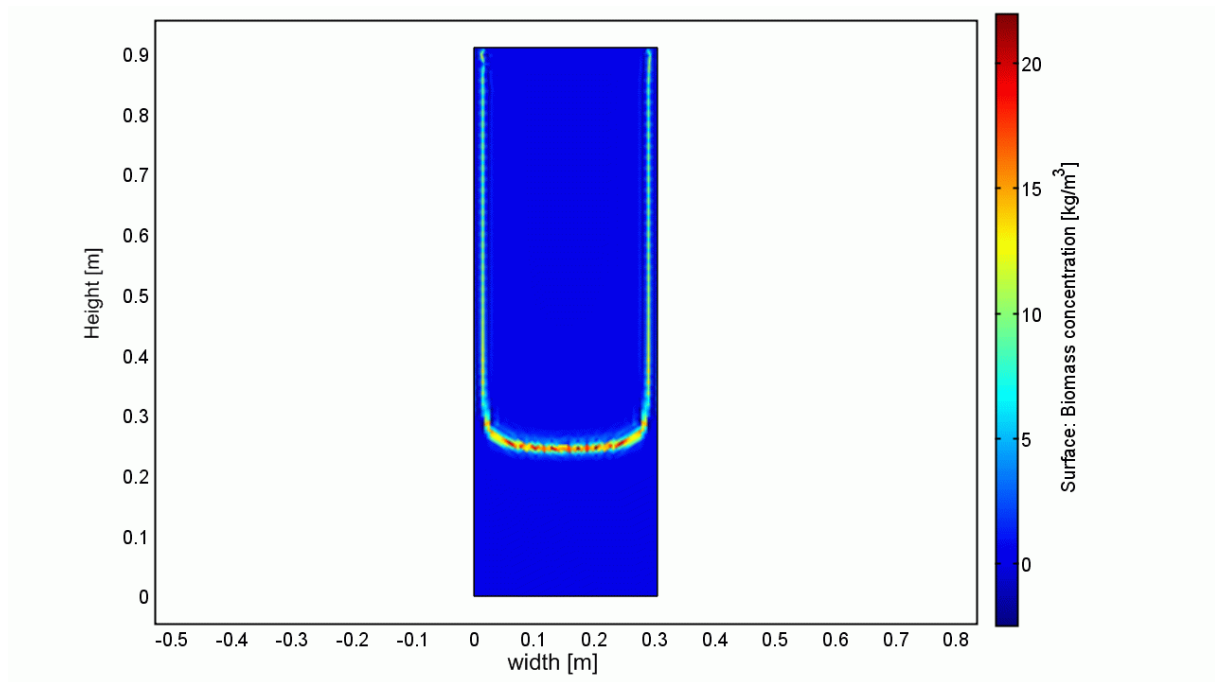


Figure 4–14: Biomass concentration resulting from a low differential pressure at the inlet ($10 Pa$) after 60 days. The pattern of concentrated biomass is shaped like a U.

a lower airflow made the areas of concentrated substrate take the shape of a filled U, the height and width of which both decreased over time.

Effects on oxygen. The composting process happened much more slowly when airflow was reduced, so that the return of the oxygen concentration to standard levels was also delayed.

Effects on water. The concentration of liquid water continuously decreased from its original value to the minimum value possible. The slow process caused the decrease to be less dramatic as compared with the regular airflow.

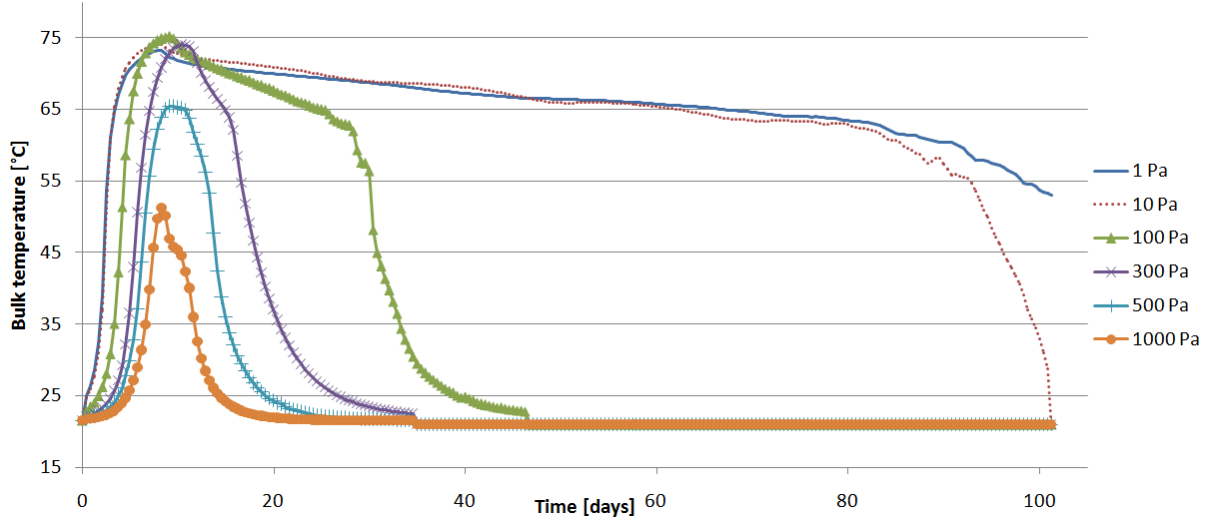


Figure 4–15: Bulk temperature in the compost for various differential pressures at the inlet.

4.3.4 Effect on the bulk temperature

Fig. 4–15 shows that a lower airflow at the inlet accelerated the composting process at first, because the heat was not evacuated as fast as with a higher airflow. The combined effects of the low supply of oxygen and low evaporation rate significantly increased the amount of time when the compost was at a high temperature.

4.4 Sensitivity analysis

4.4.1 Consumption of substrate

The analysis was performed to study the sensitivity of the airflow, the initial water content, the growth rate, and the maintenance coefficient of the biomass on the total mass of substrate at the end of the simulation. This output was chosen because the mass of substrate consumed is a good indicator of the maturity of compost.

In order to perform sensitivity analysis, the derivatives of the function giving the final mass of substrate with regard to the chosen input were obtained. This function is not algebraic and the values were computed through simulation. An algebraic expression of the derivatives was therefore unavailable. Hence, approximations of these derivatives were computed. The first derivatives were obtained with Eq. 3.43, while the second derivatives were obtained with Eq. 3.47 and 3.48.

The gradient and Hessian matrix were found to be (the components are respectively airflow, initial water concentration, μ , ν):

$$\vec{grad}(f) = \begin{pmatrix} 0.496 \\ -21.008 \\ -5.014 \\ -3.546 \end{pmatrix}; Hessian = \begin{bmatrix} -4.6 & 11.08 & 28.52 & 66.44 \\ 11.08 & 41.88 & 99.84 & 71.04 \\ 28.52 & 99.84 & 104.08 & 82.36 \\ 66.44 & 71.04 & 82.36 & 140.36 \end{bmatrix} \quad (4.1)$$

The gradient, once normalized and multiplied by the maximum perturbations for each parameter, gave the vector of the most sensitive perturbation at the first order. The first-order approximation of the effect of perturbations is linear, so the normalized gradient gives the most sensitive direction of increase in the value of the original function, while its opposite gives the most sensitive direction for decrease.

To find the second-order approximation, the function *fmincon* of MatlabTM was used with Eq. 3.46. Actually, *fmincon* was used on Eq. 3.46 and its opposite in order to find the maximum direction for the increase and decrease, in order to find the extremum. The initial point used, as required by the algorithm, was estimated from the first-order approximation, and the optimization was done under the constraint

that the normalized perturbations were located on the sphere of radius 1 in the 4-dimension space of parameters. The results are shown in Table 4–1.

Table 4–1: Sensitivity analysis results

order of approximation	perturbation	direction (in % of standard value)	final mass of substrate
first	increase	$\begin{pmatrix} 0.001133 \\ -0.047979 \\ -0.011451 \\ -0.008098 \end{pmatrix}$	42.6434 <i>kg</i>
	decrease	$\begin{pmatrix} -0.001133 \\ 0.047979 \\ 0.011451 \\ 0.008098 \end{pmatrix}$	40.5224 <i>kg</i>
second	increase	$\begin{pmatrix} -0.0002 \\ 0.9500004 \\ 0 \\ 0 \end{pmatrix}$	42.7146 <i>kg</i>
	decrease	$\begin{pmatrix} -0.00706452 \\ 0.044634917 \\ 0.016001383 \\ 0.013101472 \end{pmatrix}$	40.6490 <i>kg</i>
standard	(n/a)	$\begin{pmatrix} 0 \\ 0 \\ 0 \\ 0 \end{pmatrix}$	41.4600 <i>kg</i>

As Table 4–1 shows, the second-order approximation shows a greater positive response than the first-order. In fact, even the first-order approximation gave higher perturbations than the ones obtained when only one parameter was changed at a time. The fact that the vectors given by the first and second-order perturbations were significantly different means that there were important non-linear behaviors.

In such a situation, it is not certain that a second-order approximation is adequate, and including higher-order derivatives might be useful.

As for negative perturbations, the response was greater with the first-order approximation than with the second-order. It should be noted that the two response vectors given by these two approximations were similar. The MatlabTMfunction found a minimum for the second order response, but the constraint was not strictly respected, and the resulting vector had to be rescaled to fit in the sphere of normalized perturbation of radius 1 (its norm was initially 1.006). This may explain the fact that the second order approximation was less accurate.

CHAPTER 5

Discussion

Once again, the purpose of this model was not to be validated against any existing data. The main reason for this work is that no prior studies had included all the values for the constants or parameters required by this model. To determine all of these values experimentally, however, would have been outside of the scope of this thesis.

5.1 Multiphysics

The use of commercial software enables the easy implementation of complex physical equations, especially in fluid dynamics. The solvers of such software are constructed in order to efficiently simulate these equations with a high level of confidence. This confidence, as well as the spatial resolution and adaptability of the resulting models, makes this kind of commercial software a great tool for implementing complex simulations.

5.2 A configurable model

This model's responses were realistic, which suggests its validity. Before using the model on a larger scale, however, it should be formally validated. It is possible that the determination of the values of all the constants and parameters would be too time-consuming or difficult for the model to be usable as it is. Sensitivity analysis should then be used to point out which phenomena might be neglected and which parameters are not needed.

In this model, only one strain of biomass and one type of substrate have been modelled. It is possible, however, to represent different microbiological behavior, like mesophilic and thermophilic, by adding an equation for each strain. This modification can be easily done in COMSOLTM and requires only that one checks which equations are influenced by the addition of a microbial strain. Adding strains could have repercussions, for instance, on the equations for dissolved oxygen and heat in the liquid phase.

The partitioning of the substrate between carbonaceous and nitrogenous compound may also be accomplished by adding equations to represent the different kinds of substrate.

The production of molecules like ammonia or carbon dioxide can also be modelled by additional equations.

The model allows the possibility to define the inputs as functions of the outputs in order to represent a closed vessel.

In a physical composting system, compaction occurs. The use of COMSOLTM allows such a modification of the geometry over time and the modification of parameters, like porosity, that depend on the physical nature of the substrate can quite easily be implemented.

The possibility of adding features to the model rather than building a new makes this model an interesting tool for comparative research. In addition, building a new model often involves much debugging. Using this model as a basis for further study could save a lot of time.

5.3 Spatial dependency

The explicit spatial representation of a finite element model offers the opportunity to see behaviors that would be hard to measure during a physical experiment. This study indicated that compost processes are far from being spatially homogeneous, and some interesting features were described. Some of those features, however, may have been artifacts of the model and its limitations. For instance, in real compost, compaction may create an empty space between the walls and the compost. Thus the spatial distribution of the air velocity would be very different that seen in the simulations. Moreover, the U-shaped concentration of biomass that was shown in Fig. 4–14 was dependent on the conductive heat loss through the walls. Yet a layer of air next to the walls might change the results of the simulation: the air space might insulate the compost, or result in a preferential air flow along the walls which would have consequences elsewhere in the compost bed.

Those spatial dependencies can have an important impact on the quality of the resulting compost. The compost did not undergo the same biological processes everywhere, making it heterogeneous. The most critical areas are were those where the temperature did not rise enough to inactivate pathogens and weed seeds, and insect larvae would not have been killed by the heat. This could make the final product potentially dangerous. Turning during the composting process would help reduce the probability of survival of such organisms, but not entirely, as a small part of the compost might never be exposed to high temperatures as a result of the random mixing. It would be interesting to perform an experiment to check whether the temperature front observed to migrate vertically in simulation actually occurs in

physical systems. One way to do this would be to place several temperature probes at different depths, but taking samples of the substrate at different depths at the end of the experiment would also be feasible. If the phenomenon did occur, the option of turning the compost several times during the process would be a solution to obtaining an homogenized product.

The ability to follow spatial distributions can enable interesting experiments such as, for instance, varying the initial composition of the substrate over space by alternating layers of readily degradable and recalcitrant substrate.

5.4 Further improvements

It would be interesting to implement time-variant changes in the physical characteristics of the compost, such as porosity and compaction. Such modifications should be done carefully, since a moving mesh would be required that would increase the computation time.

The implementation of the solid phase, which would dissolve in the liquid phase, would be interesting. The dissolution of the solid might be a limiting step, especially when the consumption of dissolved substrate by the biomass was at its peak.

The physical and biological equations could be improved. One should be careful, however, not to implement a complex equation that would increase the computation time more than might be justified by any improvement to the accuracy of the results. The equations presented in this study are purported to represent all the major processes involved in composting with reasonable accuracy, while allowing a convenient simulation time. Sensitivity analysis could be performed on the equations to see which of them should be modified first. Such analysis is, however, hard to perform

for the modification of an equation because, unlike the value of a coefficient, the structure of an equation cannot be changed as a continuous variable.

5.5 Sensitivity analysis

The sensitivity analysis of the numerical model showed that the first-order approximation of the compost system was far from being sufficient, as the second-order solution was not close to the first. There was no way to ensure, however, that the second-order solution was adequate. Testing higher-order approximations would have required many simulations, probably as many as for sophisticated optimization algorithms, but it would be interesting to compare the results of this study to those that can be obtained by such algorithms. Given the necessary time and resources, the best approach would be to actually discretize the sphere of perturbations and compute the difference in output on all the discrete points of the sphere. This approach, however, would require a lot of simulations.

It would also be interesting to perform a statistical sensitivity analysis of the system. This would require a statistical study of the characteristic response of the system to a distribution of perturbations.

Efficient methods to find the extremum of a non-linear function under non-linear constraints should be used in further studies.

BIBLIOGRAPHY

- Agnew, J. and J. Leonard (2003). The physical properties of compost. *Compost Science and Utilization* 11(3), 238–264.
- Ahn, H., T. Sauer, T. Richard, and T. Glanville (2009). Determination of thermal properties of composting bulking materials. *Bioresource technology* 100(17), 3974–3981.
- Andrews, J. and K. Kambhu (1973). Thermophilic aerobic digestion of organic solid wastes. *NTIS*.
- Anonymous (2004). Waste management Industry survey: Business and Government Sectors. Statistics Canada.
- Anonymous (2005). Human Activity and the Environment. Statistics Canada.
- Anonymous (2009). Municipal Waste Treatment. United Nations Statistics Division.
- ASHRAE (2009). *2009 ASHRAE handbook fundamentals*. Atlanta, GA.: ASHRAE.
- Bender, E. A. (1978). *An introduction to mathematical modeling*. New York: Wiley.
- Benjamin, D. (2010). Recycling Myths Revisited. *PERC*.
- Berry, J. and K. Houston (1995). *Mathematical Modelling*. Modular mathematics series. London: E. Arnold.
- Bitton, G. (1998). *Formula Handbook for Environmental Engineers and Scientists*. Environmental science and technology. New York: Wiley.

- Bochner, S. (1966). *The Role of Mathematics in the Rise of Science*. Princeton, N.J.: Princeton University Press.
- Bongochgetsakul, N. and T. Ishida (2008). A new analytical approach to optimizing the design of large-scale composting systems. *Bioresource technology* 99(6), 1630–1641.
- Chandrankanthi, M., A. Mehrotra, and J. Hettiaratchi (2005). Thermal conductivity of leaf compost used in biofilters: An experimental and theoretical investigation. *Environmental Pollution* 136(1), 167–174.
- Chang, T. and C. Wen (1968). Sensitivity analysis in optimal systems based on the maximum principle. *Industrial and Engineering Chemistry Fundamentals* 7(3), 422–429.
- COMSOL AB (2008). COMSOL Multiphysics. Stockholm, Sweden. (version 3.5a).
- Crestaux, T., O. Le Maitre, and J. Martinez (2008). Polynomial chaos expansion for sensitivity analysis. *Reliability Engineering and System Safety*.
- Cussler, E. (1997). *Diffusion: Mass Transfer in Fluid Systems*. New York: Cambridge University Press.
- Cutnell, J. and K. Johnson (2005). *Cutnell & Johnson Physics* (3rd ed.). Wiley.
- Danckwerts, P. (1951). Significance of liquid-film coefficients in gas absorption. *Industrial and Engineering Chemistry* 43(6), 1460–1467.
- Diaz, L. F. (2007). *Compost Science and Technology*. Amsterdam; Boston: Elsevier.
- Dykhuisen, R. and W. Casey (1989). An analysis of solute diffusion in rocks. *Geochimica et Cosmochimica Acta* 53(11), 2797–2805.

- Dzioubinski, O. and R. Chipamn (1999). Trends in consumption and production: Selected materials.
- Ekinci, K. (2004). Modeling composting rate as a function of temperature and initial moisture content. *Compost Science and Utilization* 12, 356–364.
- Epstein, N. (1989). On tortuosity and the tortuosity factor in flow and diffusion through porous media. *Chemical engineering science* 44(3), 777–779.
- Frey, H. and S. Patil (2002). Identification and review of sensitivity analysis methods. *Risk Analysis* 22(3), 553–578.
- Gardner, R. and J. O’Neill (1981). A comparison of sensitivity analysis and error analysis based on a stream ecosystem model. *Ecological Modelling* 12(3), 173–190.
- Glancey, J. and S. Hoffman (1994). Physical properties of solid waste materials. *Paper - American Society of Agricultural Engineers*.
- Grathwohl, P. (1998). *Diffusion in Natural Porous Media : Contaminant Transport, Sorption/Desorption and Dissolution Kinetics*. Topics in environmental fluid mechanics, EFMS1. Boston: Kluwer Academic Publishers.
- Gutis, P. S. (1987). The end begins for trash none wanted.
- Hamby, D. (1994). A review of techniques for parameter sensitivity analysis of environmental models. *Environmental Monitoring and Assessment* 32(2), 135–154.
- Hamelers, H. (2004). Modeling composting kinetics: A review of approaches. *Reviews in Environmental Science and Biotechnology* 3(4), 331–342.
- Haug, R. (1993). *The Practical Handbook of Compost Engineering*. CRC.

- Higbie, R. (1935). The rate of absorption of a pure gas into a still liquid during a short time of exposure. *Transactions of the American Institute of Chemical Engineers* 31, 365-389.
- Howard, A. (1936). Manufacture of humus by the Indore process. *Nature* 137(3461), 363.
- Howard, A. (1945). *An Agricultural Testament*. Oxford University Press Oxford.
- Jeris, J. and R. Regan (1973). Controlling environmental parameters for optimum composting. *Comp. Sci* 14, 10-15.
- Johnson, J., L. Schewel, and T. Graedel (2006). The contemporary anthropogenic chromium cycle. *Environmental Science and Technology* 40(22), 7060-7069.
- Katz, J. (2002). What a waste. Federal Reserve Bank of Boston.
- Keener, H., C. Marugg, R. Hansen, and H. Hoitink (1993). *Optimizing the Efficiency of the Composting Process. Science and engineering of composting: design, environmental, microbiological and utilization aspects*. Renaissance Publications.
- Kucherenko, S., M. Rodriguez-Fernandez, C. Pantelides, and N. Shah (2008). Monte-Carlo evaluation of derivative-based global sensitivity measures. *Reliability Engineering and System Safety*.
- Lamboni, M., D. Makowski, S. Lehuger, B. Gabrielle, and H. Monod (2009). Multivariate global sensitivity analysis for dynamic crop models. *Field Crops Research* 113(3), 312 - 320.
- Levich, V. and D. Spalding (1962). *Physicochemical Hydrodynamics*. Prentice-Hall, Englewood Cliffs, NJ.

- Levins, R. (1968). *Evolution in Changing Environments; Some Theoretical Explorations*. Monographs in population biology, no. 2. Princeton, N.J.: Princeton University Press.
- Liang, Y., J. Leonard, J. Feddes, and W. McGill (2004). A simulation model of ammonia volatilization in composting. *Transactions of the ASAE* 47(5), 1667–1680.
- Lifset, R., R. Gordon, T. Graedel, S. Spatari, and M. Bertram (2002). Where has all the copper gone: The stocks and flows project, part 1. *JOM Journal of the Minerals, Metals and Materials Society* 54(10), 21–26.
- Lin, Y., G. Huang, H. Lu, and L. He (2007). Modeling of substrate degradation and oxygen consumption in waste composting processes. *Waste Management*.
- Martin, D. and G. Gershuny (1992). *The Rodale Book of Composting*. Rodale Books.
- Mason, I. (2006). Mathematical modelling of the composting process: A review. *Waste Management* 26(1), 3–21.
- Mayo, A. (1997). Effects of temperature and ph on the kinetics growth of unialga *Chlorella vulgaris* cultures containing bacteria. *Water Environment Ressources* (69), 64–72.
- Miller, F. (1989). Matric water potential as an ecological determinant in compost, a substrate dense system. *Microbial Ecology* 18(1), 59–71.
- Montgomery, R. (1947). Viscosity and thermal conductivity of air and diffusivity of water vapor in air. *Journal of Meteorology* 4(6), 193–196.
- Mu, R. and J. Leonard (1999). Measurement of air flow through MSW-sewage sludge compost. *Canadian Agricultural Engineering* 41(2), 93–97.

- Nielsen, H. and L. Berthelsen (2002). A model for temperature dependency of thermophilic composting process rate. *Compost Science and Utilization* 10(3), 249–257.
- Parr, J., R. Gardner, and L. Elliott (1981). Water potential relations in soil microbiology: proceedings of a symposium. SSSA special publication, no. 9, Madison, Wis.
- Pepper, D. and J. Heinrich (1992). *The finite element method: basic concepts and applications*. Hemisphere Pub.
- Perry, R. H. and D. W. Green (2007). *Perry's Chemical Engineers' Handbook*. New York: McGraw-Hill.
- Petric, I. and V. Selimbasic (2008). Development and validation of mathematical model for aerobic composting process. *Chemical Engineering Journal* 139(2), 304–317.
- Poulsen, T. and P. Moldrup (2007). Air permeability of compost as related to bulk density and volumetric air content. *Waste Management and Research* 25(4), 343–351.
- Ratkowsky, D., R. Lowry, T. McMeekin, A. Stokes, and R. Chandler (1983). Model for bacterial culture growth rate throughout the entire biokinetic temperature range. *Journal of Bacteriology* 154(3), 1222.
- Richard, T., H. Hamelers, A. Veeken, and T. Silva (2002). Moisture relationships in composting processes. *Compost Science and Utilization* 10(4), 286–302.
- Richard, T. and L. Walker (2006). Modeling the temperature kinetics of aerobic solid-state biodegradation. *Biotechnology progress* 22(1), 70–77.

- Robinzon, R., E. Kimmel, and Y. Avnimelech (2000). Energy and mass balances of windrow composting system. *Transactions of the ASAE* 43(5), 1253–1259.
- Rogaume, T. (2006). *Gestion des Déchets : Réglementation, Organisation, Mise en Oeuvre*. Technosup. Paris: Ellipses.
- Rosso, L., J. Lobry, and J. Flandrois (1993). An unexpected correlation between cardinal temperatures of microbial growth highlighted by a new model. *Journal of Theoretical Biology* 162(4), 447–463.
- Rynk, R. (1992). On-farm composting handbook. *New York: NRAES-54*.
- Saint-Joly, C., A. Peyre, J. Bochu, and O. N'Dao (1989). Pressure losses during ventilation of manure. *Biological Wastes* 30(2), 123–132.
- Seki, H. (2000). Stochastic modeling of composting processes with batch operation by the Fokker-Planck equation. *Transactions of the ASAE* 43(1), 169–179.
- Smith, R. and R. Eilers (1980). Numerical simulation of activated sludge composting. *USEPA*.
- Sole-Mauri, F., J. Illa, A. Magr, F. X. Prenafeta-Bold, and X. Flotats (2007). An integrated biochemical and physical model for the composting process. *Bioresource technology* 98(17), 3278–3293.
- Stombaugh, D. and S. Nokes (1996). Development of a biologically based aerobic composting simulation model. *Transactions of the ASAE* 39(1), 239–250.
- Tse, F. C. and O. C. Sandall (1979). Diffusion coefficients for oxygen and carbon dioxide in water at 25c by unsteady state desorption from a quiescent liquid. *Chemical Engineering Communications* 3(3), 147 – 153.

- Uao, P., A. Vizcarra, A. Chen, and K. Lo (1993). Composting of separated solid swine manure. *Journal of Environmental Science and Health, Part A* 28(9), 1889–1901.
- van Genuchten, M. T. (1980). A closed-form equation for predicting the hydraulic conductivity of unsaturated soils. *Soil Science Society of America* 44(5), 892–898.
- Van Ginkel, J. (1996). Physical and biochemical processes in composting material. Wageningen Agricultural University.
- Van Ginkel, J., P. Raats, and I. Van Haneghem (1999). Bulk density and porosity distributions in a compost pile. *NJAS Wageningen Journal of Life Sciences* 47(2), 105.
- Van Ginkel, J., I. Van Haneghem, and P. Raats (2002). SE-structures and environment: Physical properties of composting material: Gas permeability, oxygen diffusion coefficient and thermal conductivity. *Biosystems Engineering* 81(1), 113–125.
- Wallach, R., F. da Silva, and Y. Chen (1992). Unsaturated hydraulic characteristics of composted agricultural wastes, tuff, and their mixtures. *Soil Science* 153(6), 434.
- Wu, L. (2003). Soil water diffusion. *Encyclopedia of Water Science*, 865 – 867.
- Yu, S., O. Clark, and J. Leonard (2005). Airflow measurement in passively aerated compost. *Canadian Biosystems Engineering* 47, 6.39–36.45.